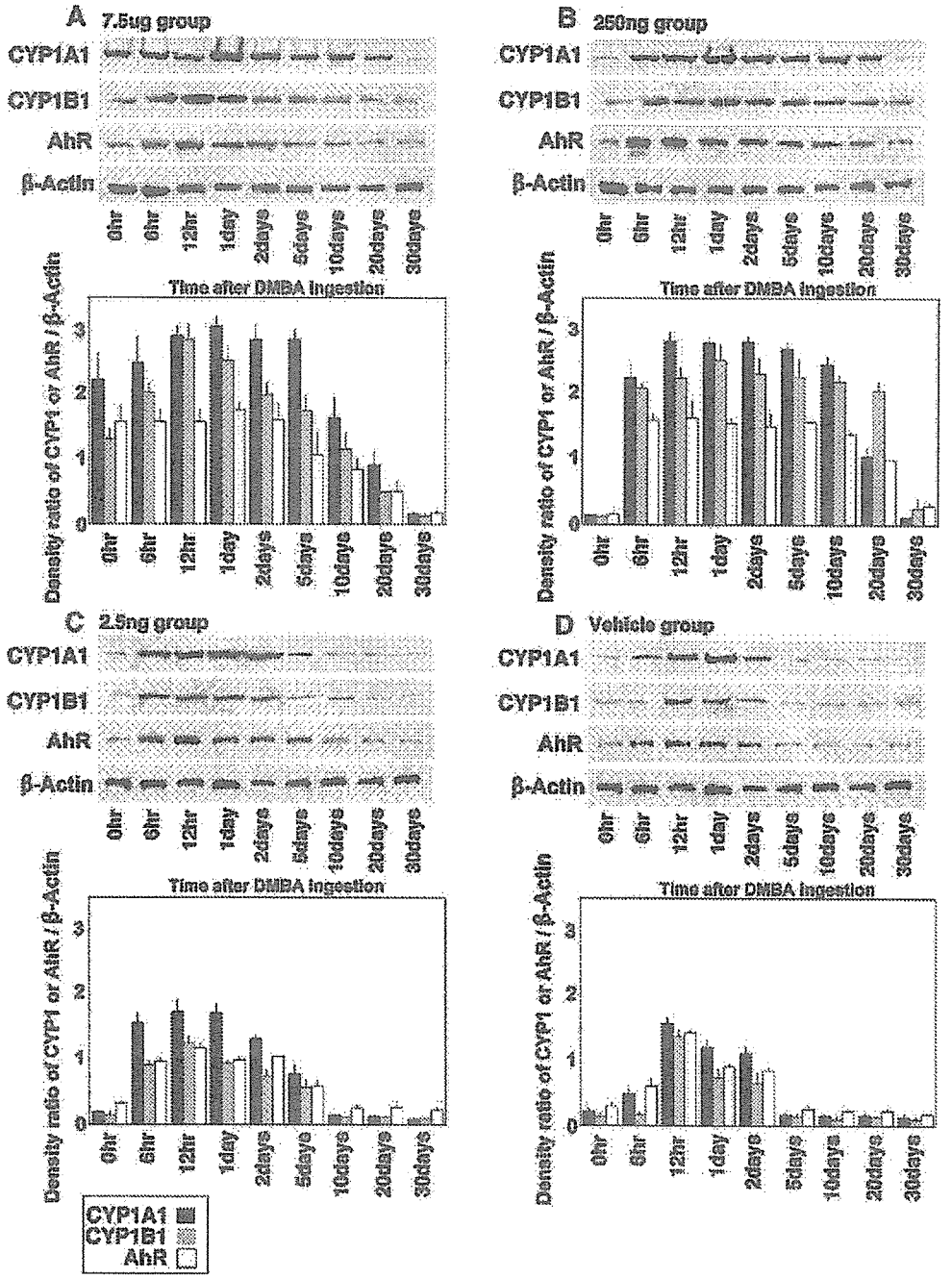

Fig. 8. Western blots of CYP1A1, CYP1B1, and AhR of rat liver following DMBA ingestion after prenatal exposure to PCB126. The protein concentration was determined with a bicinchonic acid protein assay reagent kit (Pierce) with bovine serum albumin as a standard. Ten μg of microsome samples were applied for Western blotting analysis, and immunoreactive proteins were detected using the ECL Plus Western Blotting Detection system (Amersham Biosciences, Buckinghamshire, UK). The upper panels show the representative Western blots bands of CYP1, AhR and β-actin, and the lower panels show the density ratio of CYP1, or AhR/β-actin; results are obtained by screening sample from five rats of each group. Values represent mean ± SD (A) the 7.5 μg group; (B) the 250 ng group; (C) the 2.5 ng group; (D) the vehicle group.

and liver is the primary site of E2 metabolism (Beleh et al., 1995; Waalkes et al., 2004; Wang and Liehr, 1994). This is in particular, the case of 4-hydroxylated E2, which is generated mainly by CYP1B1, displays a strong genotoxicity (Cavalieri et al., 2002; Safe and Krishnan, 1995). On the other hand, CYP1A1 generates primarily 2-hydroxylated E2, which is less toxic and has been considered as protective (Cavalieri et al., 2002; Liehr et al., 1995; Mobley et al., 1999; Schumacher et al., 1999; Yager and Liehr, 1996). Moreover, it has been suggested that the induction of mouse hepatic CYP1A1 is primarily protective for toxicity of DMBA (Uno et al., 2004). Therefore, it is possible that the prolongation of hepatic

CYP1B1 induction has been observed in the 250-ng group contributes to mammary carcinogenesis by bioactivation of both exogenous pro-carcinogens, DMBA, and endogenous E2.

A recent study showed elevated expression of AhR in the endometrium and myometrium (Khorram et al., 2002). In this study, the 250-ng group revealed elevated AhR expression compared to the other groups. Notably high levels of AhR in the liver of the 250-ng group suggest that elevated AhR expression mediated, at least in part, the increased expression of CYP1B1. As previously suggested, high levels of CYP1B1 expression, like hyperexpression of AhR, may represent a molecular marker for carcinogenesis (Spink et al., 1998). Moreover, AhR-deficient cells exhibit a decreased rate of cell proliferation because of a prolongation of cells in G1 (Ma and Whitlock, 1996; Weiss et al., 1996). The AhR also controls a number of genes whose products may be involved in a number of cellular proliferation and differentiation processes (Okey et al., 1994). In this study, because the 250-ng group showing enhancement of DMBA-induced mammary carcinogenesis revealed significantly higher AhR expression, AhR might mediate DMBA-induced mammary carcinogenesis through dysregulation of the cell cycle. However, it was unclear why a significantly lower induction of AhR was observed in the 7.5-μg group, which showed high-level PCB126 residues in mammary carcinomas, than in the 250-ng group.

Acknowledgments

The authors thank Ms. Katherine Ono for critical reading and editing of the manuscript. This study was supported by a Grant-in-Aid for High-Tech Research Center Project from the Ministry of Education, Science and Culture, Japan.

References

Angus, W.G., Larsen, M.C., Jefcoate, C.R., 1999. Expression of CYP1A1 and CYP1B1 depends on cell-specific factors in human breast cancer cell lines: role of estrogen receptor status. Carcinogenesis 20, 947–955.

Badawi, A.F., Cavalieri, E.L., Rogan, E.G., 2000. Effect of chlorinated hydrocarbons on expression of cytochrome P450 1A1, 1A2 and 1B1 and 2- and 4-hydroxylation of 17β-estradiol in female Sprague–Dawley rats. Carcinogenesis 21, 1593–1599.

Beleh, M.A., Lin, Y.C., Brueggemeier, R.W., 1995. Estrogen metabolism in microsomal, cell, and tissue preparations of kidney and liver from Syrian hamsters. J. Steroid Biochem. Mol. Biol. 52, 479–489.

Bolognesi, C., Parrini, M., Aiello, C., Rossi, L., 1991. DNA damage induced by 7,12-dimethylbenz[a]anthracene in the liver and the mammary gland of rats exposed to polycyclic aromatic hydrocarbon enzyme inducers during perinatal life. Mutagenesis 6, 113–116.

Bro-Rasmussen, F., 1996. Contamination by persistent chemicals in food chain and human health. Sci. Total Environ. 188, 45–60.

Burback, K.M., Poland, A.P., Bradfield, C.A., 1992. Cloning of the Ah receptor cDNA reveals a distinctive ligand-activated transcription factor. Proc. Natl. Acad. Sci. U.S.A. 89, 8185–8989.

Cavalieri, E.L., Balu, N., Saeed, M., Devanesan, P., 2002. Catechol ortho-quinones: the electrophilic compounds that form depurinating DNA adducts and could initiate cancer and other diseases. Carcinogenesis 23, 1071–1077.

Christou, M., Moore, C.J., Gould, M.N., Jefcoate, C.R., 1987. Induction of mammary cytochromes P-450: an essential first step in the metabolism of 7,12-dimethylbenz(*a*)anthracene by rat mammary epithelial cells. Carcinogenesis 8, 73–80.

Christou, M., Sava, U., Schroeder, S., Shen, X., Thompson, T., Gould, M., Jefcoate, C., 1995. Cytochromes CYP1A1 and CYP1B1 in the rat mammary gland: cell-specific expression and regulation by polycyclic aromatic hydrocarbons and hormones. Mol. Cell. Endocrinol. 115, 41–50.

Ciolino, H., Dankwah, M., Yeh, G., 2002. Resistance of MCF7 cells to dimethylbenz(*a*)anthracene induced apoptosis is due to reduced CYP1A1 expression. Int. J. Oncol. 21, 385–391.

Daniel, F.B., Joyce, N.J., 1984. 7,12-dimethylbenz[*a*]anthracene-DNA adduct in Sprague–Dawley and Long–Evans female rats. Carcinogenesis 5, 1021–1026.

Di Giovanni, J., Juchau, M.R., 1980. Biotransformation and bioactivation of 7,12-dimethylbenz[*a*]anthracene. Drug Metab. 11, 61–101.

Dipple, A., 1995. DNA adducts of chemical carcinogens. Carcinogenesis 16, 437–441.

Dipple, A., Moschel, R.C., Bigger, C.A.H., 1984. Polynuclear aromatic carcinogens. In: Earle, C.E.S. (Ed.), Chemical Carcinogens, 2nd ed. American Chemical Society, Washington, pp. 245–314.

Dipple, A., Khan, Q.A., Page, J.E., Ponten, I., Szeliga, J., 1999. DNA reactions, mutagenic action and stealth properties of polycyclic aromatic hydrocarbon carcinogenesis. Int. J. Oncol. 14, 103–111.

Dolwick, K.M., Schmidt, J.V., Carver, L.A., Swanson, H.J., Bradfield, C.A., 1993. Cloning and expression of a human Ah receptor cDNA. Mol. Pharmacol. 44, 911–917.

El-Bayoumy, K., Chae, Y.H., Upadhyaya, P., Meschter, C., Cohen, L.A., Reddy, B.S., 1992. Inhibition of 7,12-dimethylbenz[*a*]anthracene-induced tumors and DNA adduct formation in mammary glands of female Sprague–Dawley rats by the synthetic organoselenium compound, 1,4-phenylenebis[methylene]selenocyanate. Cancer Res. 52, 2402–2407.

Eltom, S., Larsen, M., Jefcoate, C., 1998. Expression of CYP1B1 but not CYP1A1 by primary cultured human mammary stromal fibroblasts constitutively and in response to dioxin exposure: role of the Ah receptor. Carcinogenesis 19, 1437–1444.

Evans, R.M., 1988. The steroid and thyroid hormone receptor superfamily. Science 240, 889–895.

Ginsberg, G.L., Atherholt, T.B., 1989. Transport of DNA-adducting metabolites in mouse serum following benzo(*a*)pryene administration. Carcinogenesis 10, 673–679.

Granberg, A.L., Brunstrom, B., Brandt, I., 2000. Cytochrome P450-dependent binding of 7,12-dimethylbenz[*a*]anthracene (DMBA) and benzo[*a*]pyrene (B[*a*]P) in murine heart, lung, and liver. Arch. Toxicol. 74, 593–601.

Heidel, S.M., Czuprynski, C.J., Jefcoate, C.R., 1998. Bone marrow stromal cells constitutively express high levels of cytochrome P4501B1 that metabolize 7,12 dimethlbenz[*a*]anthracene. Mol. Pharmacol. 54, 1000–1006.

Hoffman, E.C., Reyes, H., Chu, F.F., Sander, F., Conley, L.H., Brooks, B.A., Handkinson, O., 1991. Cloning of a factor required for activity of the Ah (dioxin) receptor. Science 252, 954–958.

Huggins, C., Grand, L.C., Brillantes, F.K., 1961. Mammary cancer induced by a single feeding of polynuclear hydrocarbons, and its suppression. Nature 189, 204–207.

IARC Working Group on the Evaluation of Carcinogenic Risks to Humans: Polychlorinated dibenzo-*para*-dioxins and polychlorinated dibenzofurans, 1997. IARC Monogr. Eval. Carcinog. Risks Hum. 69, 1–631.

Jones, P.B.C., Durrin, L.K., Galeazzi, D.R., Whilock, J., 1986. Control of cytochrome P-450 gene expression: analysis of a dioxin-responsive enhancer system. Proc. Natl. Acad. Sci. U.S.A. 83, 954–958.

Khorram, O., Gathwaite, M., Golos, T., 2002. Uterine and ovarian aryl

hydrocarbon receptor (AHR) and aryl hydrocarbon receptor nuclear translocator (ARNT) mRNA expression in benign and malignant gynecological conditions. Mol. Hum. Reprod. 8, 75–80.

Kothari, L., Subramanian, A., 1992. A possible modulatory influence of melatonin on representative phase I and II drug-metabolizing enzymes in 9,10-dimethyl-1,2-benzantracene-induced rat mammary tumorigenesis. Anti-Cancer Drugs 3, 623–928.

Kutz, F.W., Wood, P.H., Bottimore, D.P., 1991. Organochlorine pesticides and polychlorinated biphenyls in human adipose tissue. Rev. Environ. Contam. Toxiol. 60, 115–120.

Liehr, J.G., Ricci, M.J., Jefcoate, C.R., Hannigan, E.V., Hokanson, J.A., Zhu, B.T., 1995. 4-Hydroxylation of estradiol by human uterine myometrium and myoma microsomes: implications for the mechanism of uterine tumorigenesis. Proc. Natl. Acad. Sci. U.S.A. 92, 9220–9224.

Ma, Q., Whitlock, J.P., 1996. The aromatic hydrocarbon receptor modulates the Hepa 1c1c7 cell cycle and differentiated state independently of dioxin. Mol. Cell. Biol. 16, 2144–2150.

MacDonald, C.J., Cliolino, H.P., Yeh, G.C., 2001. Dibenzoylmethane modulates aryl hydrocarbon receptor function and expression of cytochromes P450 1A1 1B1. Cancer Res. 61, 3919–3924.

Merchant, M., Krishnan, V., Safe, S., 1993. Mechanism of action of alpha-naphthoflavone as an Ah receptor antagonist in MCF-7 human breast cancer cell. Toxicol. Appl. Pharmacol. 120, 53–63.

Mobley, J.A., Bhat, A.S., Bruggemeier, R.W., 1999. Measurement of oxidative DNA damage by catechol estrogens and analogues in vivo. Chem. Res. Toxicol. 12, 270–277.

Moon, C.J., Tricomi, W.A., Gould, M.N., 1988. Comparison of 7,12-dimethylbenz[*a*]anthracene metabolism and DNA binding in mammary epithelial cells from three rat strains with differing susceptibilities to mammary carcinogenesis. Carcinogenesis 9, 2099–2102.

Murphy, R., Harvey, C., 1985. Residues and metabolites of selected persistent halogenated hydrocarbons in blood samples from a general population survey. Environ. Health Perspect. 60, 115–130.

Murray, G.L., Taylor, M.C., McFadyen, M.C., MacKay, J.A., Greenlee, W.F., Burke, M.D., Melvin, W.T., 1997. Tumor-specific expression of cytochromes P450 CYP1B1. Cancer Res. 57, 3026–3031.

Muto, T., Wakui, S., Imano, N., Nakaaki, K., Hano, H., Furusato, M., Masaoka, T., 2001. In-utero and lactational exposure of 3,3′,4,4′,5-pentachlorobiphenyl modulate dimethylbenz[*a*]anthracene-induced rat mammary carcinogenesis. J. Toxicol. Pathol. 14, 213–224.

Muto, T., Watanabe, T., Moto, M., Okamura, M., Kashida, Y., Kanai, Y., Mitsumori, K., Endou, H., 2003. Time course of expression of 7,12-dimethylbenz[*a*]anthracene-induced CYP1A1 and CYP1B1 mRNA and protein in rat liver. J. Toxicol. Pathol. 16, 287–290.

Nandi, S., Guzman, R.C., Yang, J., 1995. Hormones and mammary carcinogenesis in mice, rat, and humans: a unifying hypothesis. Pro. Natl. Acad. Sci. U.S.A. 92, 3650–3657.

Okey, A.B., Riddick, D.S., Harper, P.A., 1994. The Ah receptor: mediator of the toxicity of 2,3,7,8-tetrachlorocibenzo-*p*-dioxin (TDCC) and related compounds. Toxicol. Lett. 70, 1–22.

Rogan, W.J., Gladen, B.C., McKinney, J.D., Carreras, N., Hardy, P., Thullen, J., Tigelstad, J., Tully, M., 1987. Polychlorinated biphenyls (PCBs) and dichlorodiphenyl dichloroethane (DDE) in human milk: effects on growth, morbidity and duration of lactation. Am. J. Publ. Health 77, 1294–1297.

Rowlands, J., He, L., Hakkak, R., Roins, M., Badger. T., 2001. Soy and whey proteins downregulate DMBA-induced liver and mammary gland CYP1 expression in female rats. Nutr. Cancer 131, 109–134.

Safe, S., Krishnan, V., 1995. Cellular and molecular biology of aryl hydrocarbon (Ah) receptor-mediated gene expression. Arch. Toxicol. 17, 99–115.

Sasaki, M., Kaneuchi, M., Fujimoto, S., Tanaka, Y., Dahiya, R., 2003. CYP1B1 gene in endometrial cancer. Mol. Cell. Endocrinol. 202, 171–176.

Schmidt, J., Bradfield, C., 1996. Ah receptor signaling pathways. Annu. Rev. Cell Dev. Biol. 12, 55–89.

Schumacher, G., Kataoka, M., Roth, J.A., Mukhopadhyay, T., 1999. Potent antitumor activity of 2-methoxyestradiol in human pancreatic cancer cell lines. Clin. Cancer Res. 5, 493–499.

Semin, B.K., Esakova, T.D., Petrusevich, I.M., Tarusov, B.N., 1976. Metabolism of 7,12-dimethylbenz(alpha)anthracene in vivo. Vopr. Onkol. 22, 54–58.

Shimada, T., Hayer, C., Yamazaki, H., Amin, S., Hecht, S., Guengerich, F., Sutle, T., 1996. Activity of chemically diverse precarinogens by human cytochrome P-450 1B1. Cancer Res. 56, 2979–2984.

Slaga, T.J., Gleason, G.L., DiGiovanni, J., Sukumaran, K.B., Harvey, R.G., 1979. Potent tumor-initiating activity of the 3,4-dihydrodiol of 7,12-dimethylbenz[*a*]anthracene in mouse skin. Cancer Res. 39, 1721–1723.

Slims, P., Grover, A., 1981. Involvement of dihydrodiols and dioepoxides in the metabolic activation of polycyclic hydrocarbons other than benzo[*a*]pyrene. In: Giboin, H.V., Ts'o, P.O.P. (Eds.), Polycyclic Hydrocarbons and Cancer, vol. 3. Academic Press, New York, NY, pp. 117–181.

Spink, D., Katz, B., Hussain, M., Pentecost, B., Cao, Z., Spink, C., 1998. Estrogen regulates Ah responsiveness in MCF-7 breast cancer cells. Carcinogenesis 24, 1941–1950.

Tanabe, S., Tatsukawa, R., Phillips, D., 1987. Mussels as bioindicators of PCB pollution: a case study on uptake and release of PCB isomers and congeners in green-lipped mussels (*Perna viridis*) in Hong Kong waters. Environ. Pollut. 47, 41–62.

Tritscher, A.M., Goldstein, J.A., Portier, C.J., McCoy, Z., Clark, G.C., Lucier, G.W., 1992. Dose-response relationships for chronic exposure to 2,3,7,8,-tetrachlorodibenzo-*p*-dioxin in a rat tumor promotion model: quantification and immunolocalization of CYP1A1 and CYP1A2 in the liver. Cancer Res. 52, 3436–3442.

Turteltaub, K.W., Felton, J.S., Gledhill, B.L., Vogel, J.S., Southon, J.R., Caffee, M.W., Finkel, R.C., Nelson, D.E., Procter, I.D., David, J.C., 1990. Accelerator mass spectrometry in biomedical dosimetry: relationship between low-level exposure and covalent binding of heterocyclic amine carcinogens to DNA. Proc. Natl. Acad. Sci. U.S.A. 87, 5288–5292.

Uno, S., Dalton, T.P., Derkenne, S., Curran, C.P., Miller, M.L., Shertzer, H.G., Nebert, D.W., 2004. Oral exposure to benzo[*a*]pyrene in the mouse: detoxication by inducible cytochrome P450 is more important than metabolic activation. Mol. Pharmacol. 65, 1225–1237.

van den Berg, M., Birnbaum, L., Bosveld, A.T.C., Brunstrom, B., Cook, P., Feely, M., Giesy, J.P., Hanberg, A., Hasegawa, R., Kennedy, S.W., Kubiak, T., Larsen, J.C., Rolaf van Leeuwen, F.X., Liem, A.K.D., Nolt, C., Peterson, R.E., Poellinger, L., Safe, S., Schrenk, D., Tillitt, D., Tysklind, M., Younes, M., Waern, F., Zacharewski, T., 1998. Toxic equivalency factors (TEFs) for PCBs, PCDDs, PCDFs for human and wildlife. Environ. Health Perspect. 106, 775–792.

Waalkes, M.P., Liu, J., Chen, H., Xie, Y., Achanzar, W.E., Zhou, Y.S., Cheng, M.L., Diwan, B.A., 2004. Estrogen signaling in livers of male mice with hepatocellular carcinoma induced by exposure to arsenic in utero. J. Natl. Cancer Inst. 96, 466–474.

Wang, M.Y., Liehr, J.G., 1994. Identification of fatty acid hydroperoxide cofactors in the cytochrome P450-mediated oxidation of estrogens to quinone metabolites. Role and balance of lipid peroxides during estrogen-induced carcinogenesis. J. Biol. Chem. 269, 284–291.

Weinberg, R.A., 1996. How cancer arises. Sci. Am. 275, 62–70.

Weiss, C., Kolluri, S.K., Kiefer, F., Gottlicher, M., 1996. Complementation of Ah receptor deficiency in hepatoma cells: negative feedback regulation and cell cycle control by Ah receptor. Ex. Cell Res. 226, 154–163.

Whitlock, J., 1999. Induction of cytochrome P4501A1. Annu. Rev. Pharmacol. Toxicol. 39, 103–125.

Yager, J.D., Liehr, J.G., 1996. Molecular mechanisms of estrogen carcinogenesis. Annu. Rev. Pharmacol. Toxicol. 36, 203–232.

J. Biochem. **139**, 761–769 (2006)
doi:10.1093/jb/mvj079

Amino Acids C-Terminal to the 14-3-3 Binding Motif in CDC25B Affect the Efficiency of 14-3-3 Binding

Sanae Uchida[1], Akitsugu Kubo[1], Ryoichi Kizu[2,*], Hitoshi Nakagama[3], Tsukasa Matsunaga[1], Yukihito Ishizaka[4] and Katsumi Yamashita[1,5]

[1]Division of Life Science and [2]Division of Environmental Science and Engineering, Graduate School of Science and Technology, Kanazawa University, Kakuma-machi, Kanazawa, Ishikawa 920-1192; [3]Biochemistry Division, National Cancer Center Research Institute, 1-1 Tsukiji 5-chome, Chuo-ku, Tokyo 104-0045; [4]Division of Intractable Disease, International Medical Center of Japan, 21-1 Toyama 1-chome, Shinjyuku-ku, Tokyo 162-8655; and [5]Cancer Research Institute, Kanazawa University, 13-1 Takara-machi, Kanazawa, Ishikawa 920-0934

Received February 8, 2006; accepted February 21, 2006

The phospho-site adapter protein 14-3-3 binds to target proteins at amino acid sequences matching the consensus motif Arg-X-X-Ser/Thr-X-Pro, where the serine or threonine residue is phosphorylated and X is any amino acid. The dual-specificity phosphatase CDC25B, which is involved in cell cycle regulation, contains five 14-3-3 binding motifs, but 14-3-3 preferentially binds to the motif at Ser309 in CDC25B1 (or Ser323 in CDC25B3). In the present study, we demonstrate that amino acid residues C-terminal to the 14-3-3 binding motif strongly affect the efficiency of 14-3-3 binding. Alanine substitutions at residues downstream of the Ser309 motif dramatically reduced 14-3-3 binding, although phosphorylation of Ser309 was unaffected. We also observed that binding of endogenous 14-3-3 to mutant CDC25B occurred less efficiently than to the wild type. Mutants to which 14-3-3 cannot bind efficiently tend to be located in the nucleus, although not as specifically as the alanine substitution mutant of Ser309. These results indicate that amino acid sequences C-terminal to the consensus binding site have an important role in the efficient binding of 14-3-3 to at least CDC25B, which may partly explain why some consensus sequences are inactive as 14-3-3 binding sites.

Key words: 14-3-3, CDC25B, cell cycle, phosphorylation, subcellular localization.

Abbreviations: CDK, cyclin-dependent kinase; GST, glutathione-S-transferase; MAPKAP, mitogen-activated protein kinase–activated protein; MK2, MAPKAP kinase 2; NLS, nuclear localization signal.

The eukaryotic cell cycle progresses through successive cycles of activation and inactivation of cyclin-dependent kinases (CDKs) that are complexed with cyclins. The activities of these complexes are regulated via several mechanisms, including inhibition of CDK by small proteins (*e.g.*, p16, p21, and p27), inhibitory phosphorylation by Wee1/Myt1 kinases at the ATP binding site of CDK, and activation of dephosphorylation by CDC25 dual-specificity phosphatases.

Three CDC25 phosphatases have been identified in mammalian cells, CDC25A, CDC25B, and CDC25C (*1*). The first CDC25 phosphatase gene to be identified was that encoding CDC25C, which dephosphorylates phospho-Tyr15 of CDK1 (previously phosphorylated by Wee1 kinase) to promote the G2 to M phase transition (*2*, *3*). Studies using cultured mammalian cells have suggested that CDC25A plays a role in the G1 to S phase transition by activating CDK2/cyclin E (*4*, *5*), and that CDC25B and CDC25C function in M phase entry by activating and maintaining CDK1:cyclin B activity during the M phase (*6–9*).

*To whom correspondence should be addressed at the present address: Department of Environmental Biochemistry, Faculty of Pharmaceutical Sciences, Doshisha Women's College of Liberal Arts, Kodo, Kyotanabe 610-0395. Tel: +81 76 264 5809, Fax: +81 76 264 5989, E-mail: katsumi@kenroku.kanazawa-u.ac.jp

Recent reports provided evidence that CDC25A also plays an important role in the G2 to M phase transition, thus indicating that CDC25A regulates all cell cycle stages (*10*, *11*). However, mice depleted of CDC25C by gene targeting develop normally and become fertile adults (*12*), and CDC25B knockout mice are born essentially healthy, although the females are sterile because of a defect in oogenesis (*13*). A recent report confirmed that mice lacking both the CDC25B and CDC25C genes are born healthy and that cells derived from these mice not only undergo normal entry to the M phase but also exhibit no checkpoint defects (*14*). Therefore, CDC25B and CDC25C are not essential for mouse development and for DNA damage checkpoints.

CDC25 proteins are CDK activators and, as a result, may comprise important cell cycle checkpoints (*15–17*). When the cell cycle checkpoint kinase CHK1 or CHK2 is activated by genotoxic stress, it phosphorylates several serine or threonine residues in CDC25A, which leads to the ubiquitin-proteasome pathway-mediated degradation of CDC25A that accompanies cell cycle arrest at the G1, G2, or intra-S phase (*10*, *17*). CDC25B and CDC25C, as well as CDC25A, are good substrates for CHK1 and CHK2 *in vitro* (*18–20*). CDC25B overexpression overrides the G2 checkpoint after ionizing radiation and other genotoxic stresses, and overproduction of a non-phosphorylated

mutant form of CDC25C partially overrides the G2 checkpoint (*21–24*).

One of the phospho-site adapter proteins, 14-3-3, appears to be centrally involved in the CDC25 function, especially in terms of checkpoint function (*15, 22–25*). CHK1 and CHK2 [and very recently mitogen-activated protein kinase-activated protein (MAPKAP) kinase 2 (MK2)] have been shown to phosphorylate CDC25B and CDC25C at phosphorylation sites containing the 14-3-3 consensus binding sequence (*23, 24, 26*). The binding of 14-3-3 to CDC25B or CDC25C may recruit these phosphatases to the cytoplasm from the nucleus and help to retain them there, thus preventing CDK1 activation in the nucleus (*27–30*). However, CDC25 phosphorylation by CHK1 or CHK2 down-regulates its phosphatase activity, in both 14-3-3 binding–dependent and –independent manners (*31–33*). At this point, the precise role of CDC25 binding to 14-3-3 in the normal cell cycle and its checkpoints remains to be defined.

We previously reported that 14-3-3β and 14-3-3ε can bind to Ser309 phosphorylation site in CDC25B1, and that the single phosphorylation at Ser309 is sufficient to sustain the binding of the β and ε 14-3-3 isoforms (*30*). In the present study, we further examined the importance of 14-3-3 binding in the regulation of CDC25B. We studied binding to CDC25B of other 14-3-3 isoforms, such as 14-3-3γ, η, θ, which is also called τ, and ζ and found that they bind primarily to the Ser309 site. Furthermore, our results reveal major roles not only for the amino acids in the Ser309 consensus site but also for the amino acids surrounding the consensus site in efficient 14-3-3 binding.

EXPERIMENTAL PROCEDURES

Cell Culture and Transformation—HEK293, Cos-7, and HeLa cells (American Type Culture Collection strains CRL-1573, CRL-1651, and CCL-2, respectively) were grown in Dulbecco's Modified Eagle's Medium supplemented with 10% fetal bovine serum, 100 μg/ml penicillin, 100 U/ml streptomycin, and 50 μg/ml M-Plasmocin under a humidified atmosphere of 5% CO_2. Fetal bovine serum, penicillin, and streptomycin were from Sigma (St. Louis, MO, USA), and M-Plasmocin from Invivogen (San Diego, CA, USA). For the transformation of HEK-293 and Cos-7 cells, appropriate amounts of DNA were transfected with FuGENE6 (Roche Diagnostics, Indianapolis, IN, USA). HeLa cells were transfected with LipofectAMINE2000 (Invitrogen, Carlsbad, CA, USA) according to the manufacturer's recommendation.

Plasmid Construction—Plasmids encoding N-terminal double FLAG-tagged CDC25B1, and N-terminal double myc-tagged 14-3-3β, ε, and σ were constructed as described previously (*30*). For the isolation of the other 14-3-3 subtypes, the coding regions were amplified by PCR using specific primers for 14-3-3γ, η, θ, and ζ. Each amplified fragment was subcloned into a modified pEF6-mycHisB vector (Invitrogen) such that a double Myc-tag was encoded at each N-terminus. The sequences of these primers are shown in Table 1. Human CHK1 and CHK2 were provided by Steve Elledge of Harvard Medical School. Human MK2 cDNA was purchased from Open Biosystems (Huntsville, AL, USA). All were amplified with specific primers (Table 1) and subcloned into modified pEF6-mycHisB such that a double HA tag was encoded at the N- or C-terminus and a 6×His tag was encoded at the C-terminus. The GST-CDC25B peptide expression plasmid was constructed by PCR amplification of the CDC25B gene, digestion of the PCR product with *Nco*I and *Xho*I, and ligation into the pGEX-KG vector (*34*). The primers used to amplify CDC25B are shown in Table 1.

Site-Directed Mutagenesis—PCR-based site-directed mutagenesis with complementary oligonucleotide pairs was used to insert alanine point mutations in CDC25B, and to place a *Bam*HI restriction site between Leu319 and Lys320 of CDC25B. The sequence of one strand of each primer pair is shown in Table 2.

Antibodies—Antisera against a phospho-Ser309 peptide (*23*) and the FLAG tag (*35*) were raised as described and affinity purified. Anti-myc and anti-HA antibodies were from Cell Signaling (Beverly, MA, USA), anti-GST

Table 1. **PCR primers used for amplification and construction of tagged proteins.**

Gene	Primer	DNA sequence (5′→3′)
14-3-3γ	Forward	AGCCCCGGATCCATGGTGGACCGCGAGCAACTGGTG
	Reverse	TCCCCTGAATTCTTAATTGTTGCCTTCGCCGCCATC
14-3-3η	Forward	CCGAGCCGGATCCCATATGGGGGACCGGGAGCAGCTGCTG
	Reverse	CCTGAAGAATTCTCAGTTGCCTTCTCCTGCTTCTTC
14-3-3θ	Forward	CCCGCGGGATCCATGGAGAAGACTGAGCTGATCCAG
	Reverse	ACACCCGAATTCGATTTAGTTTTCAGCCCCTTCTGC
14-3-3ζ	Forward	GAACATGGATCCATGGATAAAAAATGAGCTGGTTCAG
	Reverse	AAGTTGGAATTCCGGTTAATTTTCCCCTCCTTCTTC
CHK1	Forward	CTCGGTCTAGACATGGCAGTGCCCTTTGTG
	Reverse	GCCGATGGTGATATCATGTGGCAGGAAGCC
CHK2	Forward	GCTCACGGTACCGCCATGTCTCGGGAGTCG
	Reverse	TTCAAACCACGGGATATCCAACACAGCAGC
MK2	Forward	TCCCCGGGTACCATGCTGTCCAACTCCCAGGGCCAG
	Reverse	CGCGGTGATATCGTGGGCCAGAGCCGCAGCCTCCAGGG
MKK6	Forward	AAGGGGCATATGTCTCAGTCGAAAGGCAAGAAGCGAAACCCTGGC
	Reverse	GTCCACGATATCTTAGTCTCCAAGAATCAGTTTTACAAAAGATGC
GST-CDC25B	Forward	GTTCCCCCAGCCATGGAGAGTCTCATTAGT
	Reverse	TGATTTTGACTCGAGCTAGCGGGCTTTAGG

Table 2. **Sequences of primer pairs used for PCR-based site-directed mutagenesis of CDC25B.**

Mutation	Forward primer sequence (5′→3′)
Leu304Ala	AAGTGCCAGCGGGCCTTCCGCTCTCCG
Arg306Ala	CAGCGGCTCTTCGCCTCTCCGTCCATG
Ser309Ala	CTCTTCCGCTCTCCGGCCATGCCCTGCAGC
Met310Ala	CGCTCTCCGTCCGCCCCCTGCAGCGTG
Pro311Ala	TCTCCGTCCATGGCCTGCAGCGTGATC
Cys312Ala	CCGTCCATGCCCGCCAGCGTGATCCGG
Ser313Ala	TCCATGCCCTGCGCCGTGATCCGGCCC
Val314Ala	ATGCCCTGCAGCGCCATCCGGCCCATC
Ile315Ala	CCCTGCAGCGTGGCCCGGCCCATCCTC
Arg316Ala	TGCAGCGTGATCGCTCCCATCCTCAAG
Pro317Ala	AGCGTGATCCGGGCCATCCTCAAGAGG
Ile318Ala	GTGATCCGGCCCGCCCTCAAGAGGCTG
Leu319Ala	ATCCGGCCCATCGCCAAGAGGCTGGAG
319/BamHI/320	CGGCCCATCCTCGGATCCAAGAGGCTGGAG

serum from Amersham Biosciences (Piscataway, NJ, USA), and anti-FLAG M2-beads from Sigma.

Preparation of Cell Extracts, Immunoprecipitation, and Immunoblotting—Crude cell extracts were prepared as described previously (*30*). Cells were collected by scraping, washed in ice-cold phosphate-buffered saline (PBS), and lysed with immunoprecipitation (IP) buffer (50 mM Tris-HCl, pH 7.5, 150 mM NaCl, 0.5% NP-40, 5 mM EGTA, and 1 mM EDTA) supplemented with protease and phosphatase inhibitor mixes as described previously (*30*). Cell extracts were centrifuged at 15,000 ×*g* for 10 min at 4°C, the supernatant fractions were collected, and the protein concentrations were determined by the Bradford method (Bio-Rad, Richmond, CA, USA) (*36*). For immunoprecipitation, typically 500 μg of protein was mixed with anti-FLAG M2-agarose beads or 2 μg of anti-myc monoclonal antibodies followed by protein G-Sepharose beads (Amersham Biosciences). Crude cell extracts or immunoprecipitates were subjected to immunoblotting using rabbit polyclonal anti-FLAG antibodies (for CDC25B), mouse monoclonal anti-myc antibodies (for 14-3-3), or mouse monoclonal anti-HA antibodies (for kinases).

Protein Purification—Protein kinases were prepared from cDNA-transfected Cos-7 cells. Typically, 8×10^5 Cos-7 cells in a 6-cm dish received 4 μg of plasmid DNA with FuGENE6. After 24 h, the cells were collected, washed with PBS, and lysed with EDTA-free IP buffer supplemented with a 1:100 dilution of FOCUS Protease Arrest (EMD Biosciences, San Diego, CA, USA), 20 mM *p*-nitrophenyl phosphate, 20 mM NaF, and 20 mM β-glycerophosphate. To purify the kinases, Ni^{2+}-charged immobilized metal-chelating Sepharose beads (Amersham Biosciences) were added to the cell extracts containing 1.5 mg protein, and the protein-bound beads were used directly in kinase assays. GST-tagged proteins were expressed in *Escherichia coli* BL21 (DE3) cells transformed with the appropriate cDNA plasmid constructs. Expression was induced with 0.4 mM isopropyl-β-D-thiogalactopyranoside, and proteins were purified with glutathione–Sepharose beads (Amersham Biosciences).

Indirect Immunofluorescence Microscopy—Indirect immunofluorescence analysis was performed as described previously (*30*, *37*). Transfected HEK293 cells were fixed with 3.7% formaldehyde and then permeabilized with 0.5% Triton X-100. Expressed CDC25B proteins were detected with rabbit polyclonal anti-FLAG antibodies, followed by AlexaFluor 594– or 488–conjugated goat anti-rabbit IgG (Molecular Probes, Eugene, OR, USA), and expressed 14-3-3 was detected with mouse monoclonal anti-Myc antibodies and AlexaFluor 488–conjugated goat anti-mouse IgG. Nuclei were stained with 4′,6-diamino-2-phenylindole (Sigma).

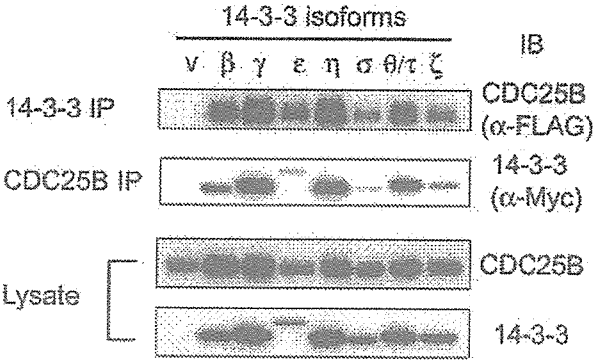

Fig. 1. **Binding of 14-3-3 subtypes to CDC25B.** HEK293 cells (1.4×10^6 cells per 35-mm plate) were transfected with 3 μg of FLAG-tagged CDC25B DNA and 0.6 μg of myc-tagged 14-3-3 DNA. The cells were collected 24 h after transfection, and cell extracts were prepared. The cell extracts were either subjected to Western blotting to visualize protein expression or further processed for immunoprecipitation with anti-FLAG or anti-myc antibodies to analyze binding. Upper panel: IP with anti-myc (14-3-3), followed by IB with anti-FLAG (CDC25B); second panel: IP with anti-FLAG (CDC25B), followed by IB with anti-myc (14-3-3).

RESULTS

All Seven Isoforms of 14-3-3 Bind to CDC25B—We previously showed that 14-3-3 isoforms β, ε, and σ bind efficiently to CDC25B, with the β and ε isoforms binding preferentially to the 14-3-3 binding motif at Ser309 (309 site), and the σ isoform binding preferentially to the motif at Ser216 (216 site) (*30*). In the present study, we analyzed the binding properties of four additional isoforms of 14-3-3. The genes for the γ, η, θ, and ζ isoforms were amplified by PCR and expressed in HEK293 cells. Each 14-3-3 isoform was co-expressed with CDC25B, isolated, and analyzed as to its interaction with CDC25B. As shown in Fig. 1, all the14-3-3 isoforms were able to interact with CDC25B. CDC25B was detected in immunoprecipitates of all the 14-3-3 isoforms (Fig. 1, upper panel), and all the 14-3-3 isoforms were recovered in the CDC25B co-immunoprecipitates (Fig. 1, second panel). Taking the protein expression levels into account, the 14-3-3ε, σ, and ζ isoforms appeared to bind more weakly to CDC25B than did the other 14-3-3 isoforms (Fig. 1, second and fourth panels).

As we reported previously (*30*), CDC25B has five 14-3-3 consensus binding motifs (Fig. 2A). Here, we examined the CDC25B binding site preference of each 14-3-3 isoform using co-transfection with plasmids encoding various CDC25B mutants. Five of these mutants contained

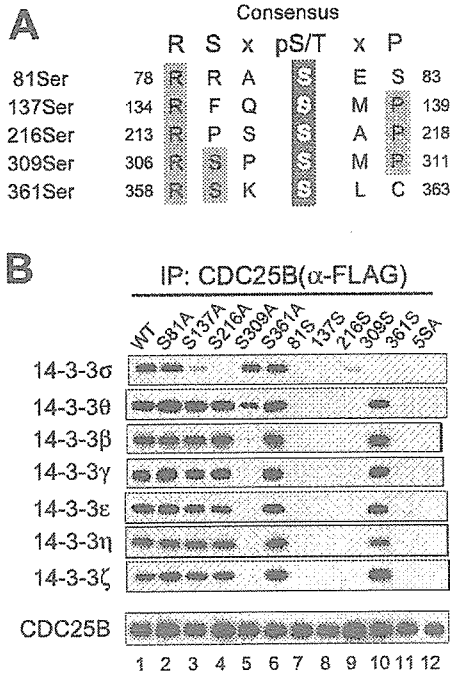

C

14-3-3 subtype	CDC25B mutants											
	WT	S61A	S137A	S216A	S309A	S361A	81S	137S	216S	309S	361S	5SA
σ	++	++	+	–	++	++	–	–	±	–	–	–
θ	++	++	++	++	+	++	–	–	–	++	–	–
β	++	++	++	++	–	++	–	–	–	++	–	–
γ	++	++	++	++	±	++	–	–	–	++	–	–
ε	++	++	++	++	±	++	–	–	–	++	–	–
η	++	++	++	++	–	++	–	–	–	++	–	–
ζ	++	++	++	++	±	++	–	–	–	++	–	–

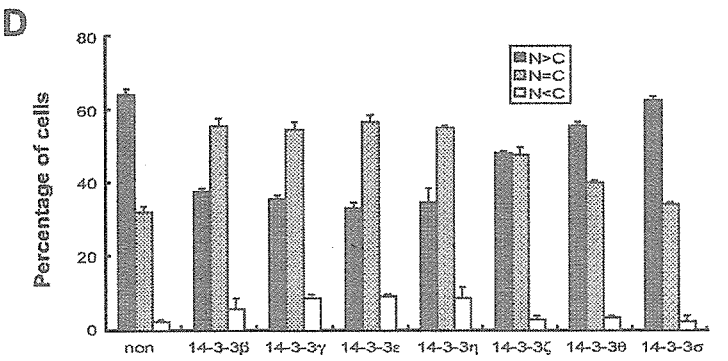

Fig. 2. **CDC25B binding site preferences of 14-3-3 subtypes.** FLAG-tagged CDC25B mutants with Ser→Ala substitutions at possible 14-3-3 binding sites (*30*) were co-transfected with each 14-3-3 subtype, as described in Fig. 1. Cell extracts were prepared 24 h after transfection and then immunoprecipitated with anti-FLAG-agarose beads to recover the CDC25B mutant proteins. Recovered CDC25B and co-immunoprecipitated 14-3-3 were detected by Western blotting. A: Possible 14-3-3 consensus binding sites and their amino acid sequences. B: Isoforms of 14-3-3 recovered with anti-FLAG-agarose beads. The bottom panel indicates a typical result of expression of co-transfected CDC25B mutants. C. Summary of the results shown in B. ++, strong signal; +, moderate signal; ±, discernible after long exposure; –, no signal. D. Subcellular localization of wild-type CDC25B upon co-expression with 14-3-3 subtypes. Cover slips in 35-mm plates were seeded with 2×10^5 HEK293 cells. After 2 days, the cells were transfected with myc-tagged 14-3-3 subtypes in combination with FLAG-tagged wild-type CDC25B. The cells were fixed 24 h after transfection, and the subcellular localization of CDC25B was determined by staining with anti-FLAG antibodies. More than 200 cells were examined. The data shown are the averages of three independent experiments. Bars = standard deviation.

single-site Ser→Ala substitutions in one 14-3-3 binding motif (*e.g.*, mutant Ser309Ala). In addition, the 309Ser mutant contained Ser→Ala substitutions at all possible binding sites except site 309, and the 5SerAla mutant contained Ser→Ala substitutions at all five putative binding sites.

CDC25B immunoprecipitates were recovered from cells co-transfected with the *14-3-3* and mutant *CDC25* genes, and 14-3-3 was detected on Western blots. All 14-3-3 isoforms except 14-3-3σ were found to bind preferentially to site 309 (Fig. 2B), as shown previously (*30*). Although substantial binding of 14-3-3θ to the Ser309Ala mutant did occur, comparison with the other single-site mutations revealed that 14-3-3θ bound preferentially to site 309. These results are summarized in Fig. 2C.

We examined the effect of co-transfection with 14-3-3 isoforms on the subcellular localization of CDC25B. Previously, we found that the binding of 14-3-3 at site 309 caused CDC25B to move from the nucleus to the cytoplasm (*30*). In the present study, we found that 14-3-3 isoforms that preferentially bound at site 309 caused CDC25B to be exported from the nucleus to the cytoplasm, and that isoforms that bound weakly or non-preferentially to site 309 did not have such an effect (Fig. 2D). The 14-3-3θ isoform, which binds preferentially to site 309, exhibited a mobilizing effect on the 309Ser mutant (data not shown), consistent with the results of the binding analysis above.

Mutations Near Ser309 of CDC25B Interfere with 14-3-3 binding—The effects of co-transfection with 14-3-3 on the cytoplasmic distribution of CDC25B indicated that 14-3-3 binding at site 309 may have masked the nuclear localization signal (NLS) sequence of CDC25B, which begins about ten residues downstream of the binding site (Fig. 3A). We therefore conducted experiments to determine the effect of an increased distance between Ser309 and the NLS sequence. Lys320 is the first residue of the bipartite NLS sequence in CDC25B. To enable the in-frame insertion of additional amino acids, we initially used mutagenesis to introduce a *Bam*HI site between residues 319 and 320. The *Bam*HI recognition sequence resulted in the insertion of Gly–Ser (GS) dipeptide immediately before Lys320 (Fig. 3A). We found, however, that this GS insertion abolished 14-3-3 binding to CDC25B, despite the fact that phosphorylation at site 309 was detected with phospho-Ser309 antibodies (Fig. 3B).

These results were intriguing because there have been no previous reports that amino acid sequences C-terminal

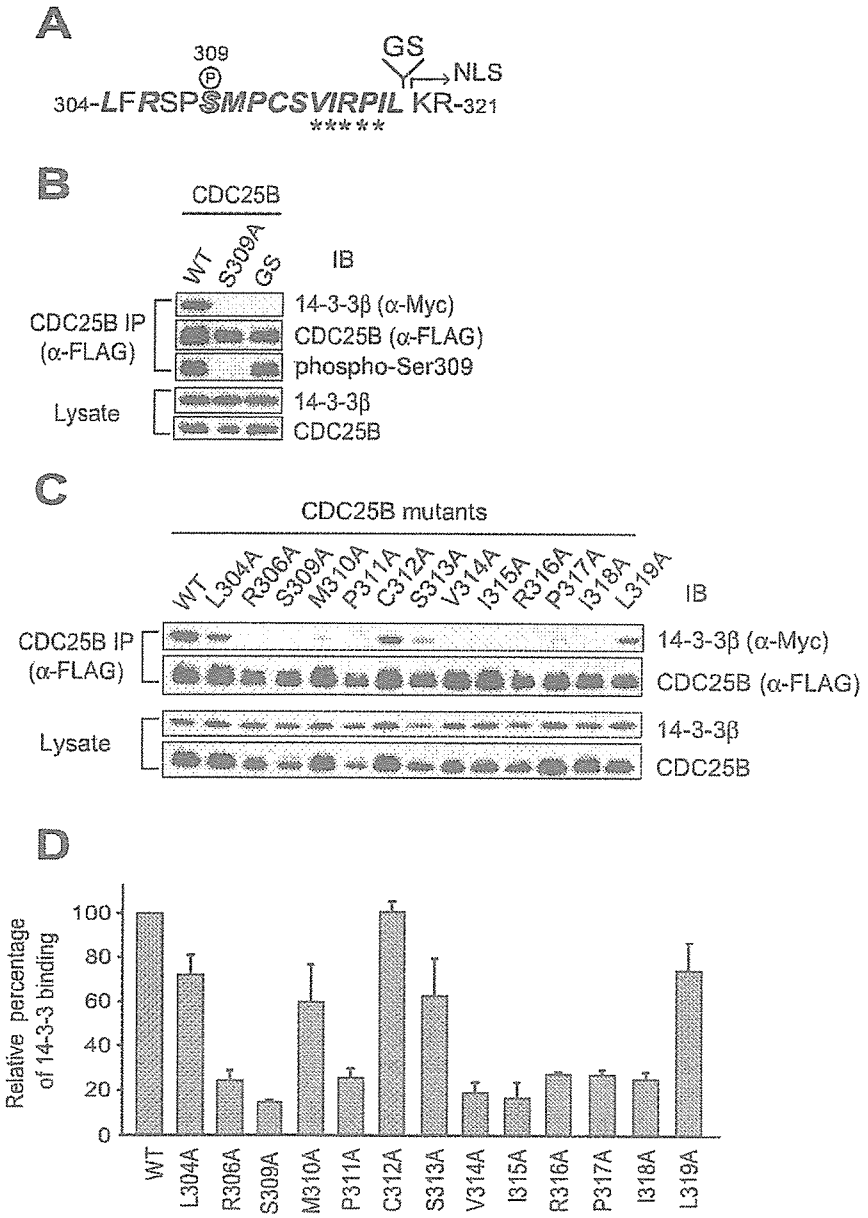

Fig. 3. **Binding of 14-3-3β to CDC25B mutants with substitutions near Ser309.** CDC25B mutants containing point substitutions near Ser309 were co-transfected with 14-3-3β, and CDC25B mutant proteins were isolated with anti-FLAG-agarose beads as described in Fig. 2. CDC25B-bound 14-3-3β was identified with an anti-myc antibody. A. Amino acid sequence from Leu304 to Arg321. Ser309 is denoted by an outlined letter S. A *Bam*HI site (GGATCC), which encodes Gly–Ser, was inserted between Leu319 and Lys320. Lys320 is the N-terminal end of the NLS sequence in CDC25B, which is indicated by an arrow. Bold italic letters indicate amino acids changed to Ala to analyze 14-3-3 binding, the results of which are depicted in (C) and (D). Asterisks indicate the hydrophobic amino acid stretch (see text). The GS insertion mutant (+ GS in B) and a series of point mutants (C) of CDC25B were analyzed as to their binding to 14-3-3β and the phosphorylation of Ser309, which was determined with anti-phospho-Ser309 antibodies. The efficiency of 14-3-3β binding to each CDC25B mutant relative to wild-type CDC25B was calculated from the data presented in (C) and is depicted in (D). The data shown are the averages of three independent experiments. Bars = standard deviation.

to the 14-3-3 binding site affect the interaction between 14-3-3 and its target proteins. We further examined this phenomenon by introducing single alanine point mutations at residues 304 to 319 of CDC25B, and then co-transfecting the resulting mutants and 14-3-3β (indicated by bold italic letters in Fig. 3A). Surprisingly, all of the tested point mutations except Cys312Ala and Leu319Ala caused a diminished interaction with 14-3-3 (Fig. 3C). The results clearly demonstrate that the hydrophobic amino acid region from Val315 to Ile318 seems to be important for 14-3-3 binding (Fig. 3D and depicted by asterisks in Fig. 3A). Pro311 of CDC25B, which is part of the 14-3-3 binding consensus sequence, also appeared to be important for 14-3-3 binding. Thus, alterations in the amino acids near the core consensus sequence of site 309 of CDC25B negatively affected its ability to bind to 14-3-3.

Ser309 Phosphorylation by Several Candidate Kinases—To study the *in vivo* phosphorylation of Ser309 in these mutants, we transfected some of the mutant *CDC25B* genes, and the mutant proteins were recovered and assayed for phosphorylation at Ser309. As shown in Fig. 4A, phosphorylation of Ser309 occurred in all of the mutants expressed in HEK293 cells, except for the Pro317Ala mutant expressed in Cos-7 cells.

Several kinases that phosphorylate Ser309 of CDC25B1 (or Ser323 of CDC25B3) have been reported. We attempted to determine which kinases could phosphorylate the CDC25B mutants. We expressed candidate kinases

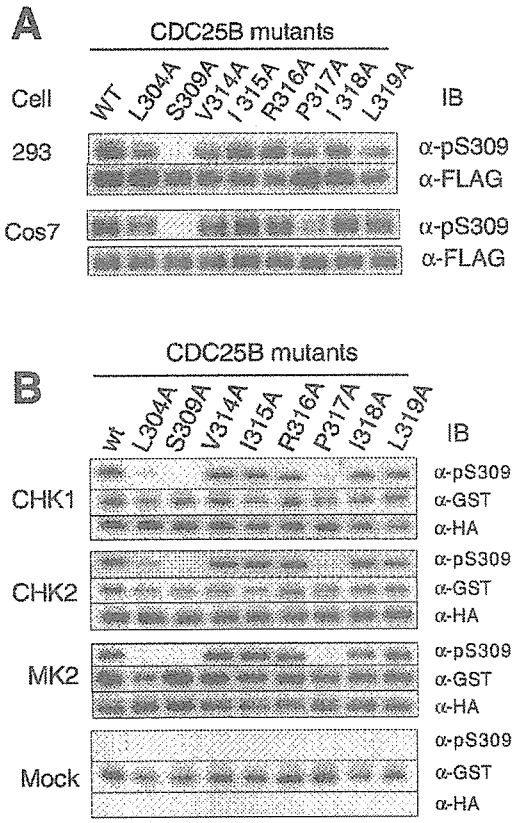

Fig. 4. **Phosphorylation of Ser309 *in vivo* and *in vitro* by representative kinases.** HEK293 cells (1.4×10^6 cells per 35-mm plate) or Cos-7 cells (2×10^5 cells per 35-mm plate) were transfected with plasmids carrying FLAG-tagged CDC25B mutants, and the expressed proteins were immunoprecipitated with monoclonal anti-FLAG beads. The precipitated proteins were immunoblotted with anti-FLAG or anti-phospho-Ser309 antibodies (A). His- and HA-tagged kinases were expressed in Cos-7 cells and recovered as described. The recovered kinases were incubated with GST-fused CDC25B peptides (wild-type or mutant), and phosphorylation at Ser309 was determined by immunoblotting (B).

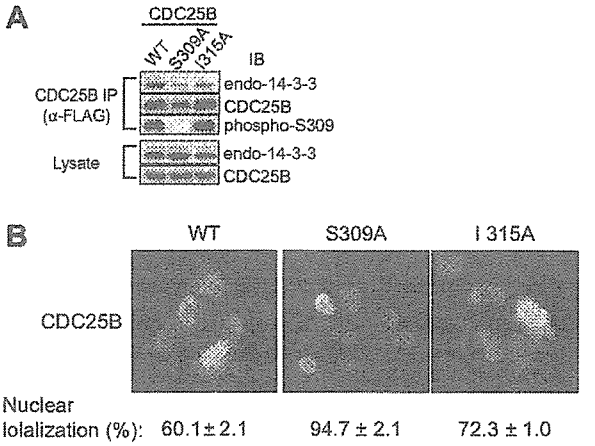

Fig. 5. **Binding of endogenous 14-3-3 to CDC25B mutants and subcellular localization.** HEK293 cells were transfected with plasmids carrying wild type CDC25B or Ala309 or Ala315 mutants, and the expressed proteins were recovered with anti-FLAG beads. The precipitates were immunoblotted with an anti-pan 14-3-3 antibody (upper panel), anti-FLAG antibody (second panel), or anti-phospho-Ser309 antibody (third panel). The expression of endogenous 14-3-3 and transfected CDC25B is indicated in the two bottom panels (A). HEK293 cells were transfected with CDC25B plasmids as in (A), and the subcellular localization of the expressed CDC25B proteins was determined as in Fig. 2D. The numbers represent the percentages of cells expressing the CDC25B protein found exclusively in the nucleus. Three independent experiments were performed for each value , and more than 200 CDC25B-expressing cells were counted in each experiment (B).

CHK1 (*18*), CHK2 (*19*) and MK2 (*26*) in Cos-7 cells and then recovered the kinases by immunoprecipitation. For the preparation of MK2, an upstream kinase, mitogen-activated protein kinase kinase kinase 6 (MKK6) and MK2 were co-transfected, and the expressed MK2 was immunoprecipitated. An *in vitro* phosphorylation assay indicated that the three kinases could phosphorylate GST-tagged CDC25B mutant peptides (Fig. 4B), the results being similar to those obtained *in vivo* (Fig. 4A). The kinases phosphorylated all of the mutant peptides with similar efficiency, with the exception of the Pro317Ala mutant, consistent with the results shown in Fig. 4A. These results demonstrate that Ser309 of CDC25B can be phosphorylated by several kinases.

Binding of Endogenous 14-3-3 to CDC25B Mutants and Their Subcellular Localization—We examined the binding of endogenous 14-3-3 to mutant CDC25B proteins. After transfection to HEK293 cells, CDC25B proteins were recovered, and the bound 14-3-3 protein was quantitated using a pan-14-3-3 antibody. Figure 5A shows that the efficiency of endogenous 14-3-3 binding to mutant CDC25B was similar to that in the co-expression experiments. Endogenous 14-3-3 bound to wild-type CDC25B most efficiently and to the 309Ala mutant least efficiently. A lesser amount of endogenous 14-3-3 was detected with the 315Ala mutant, which exactly matched the results in Fig. 3C and D. The phosphorylation of S309 in the I315A mutant could also be reproduced (compare Figs. 5A and 4A). We examined the subcellular localization of these mutant CDC25B proteins expressed in cells (Fig. 5B). The number of cells with CDC25B specifically localized in the nucleus was higher for mutant CDC25B than for the wild-type protein. About 72% of the cells exhibited specific nuclear localization of CDC25B 315Ala mutants, which was higher than the frequency of nuclear localization of wild-type CDC25B (~60%). Collectively, amino acid sequences surrounding the 14-3-3 binding core consensus site have a strong influence on 14-3-3 binding but subcellular localization of CDC25B can not be simply explained by 14-3-3 binding.

Finally, the results of this study are summarized in Table 3.

DISCUSSION

Seven isoforms of 14-3-3 have been identified in mammalian cells. We previously reported that three isoforms, 14-3-3β, ε, and σ, are able to bind to CDC25B, and that the

Table 3. **Summary of 14-3-3β binding and Ser309 phosphorylation of each CDC25B mutant.**

Name	Sequence	14-3-3β Binding (%)	Ser309 phosphorylation	
			in vivo	*in vitro*
WT	^{304}LFRSPSMPCSVIRPILKR^{321}	100	+	+
GS	LFRSPSMPCSVIRPILGSKR	17	+	NT
L304A	A----------KR	70	+	±
R306A	--A----------KR	23	NT	NT
S309A	-----A----------KR	18	–	–
M310A	------A---------KR	60	NT	NT
P311A	-------A--------KR	25	NT	NT
C312A	--------A-------KR	103	NT	NT
S313A	---------A------KR	63	NT	NT
V314A	----------A-----KR	21	+	+
I315A	-----------A----KR	17	+	+
R316A	------------A---KR	27	+	+
P317A	-------------A--KR	27	+	±
I318A	--------------A-KR	25	+	+
L319A	---------------AKR	72	+	+

binding site for 14-3-3β and ε is different from that for 14-3-3σ. Moreover, after binding to 14-3-3β or ε but not σ, CDC25B is exported to the cytoplasm. The recently published X-ray structure results revealed the following specific functional and structural features of the 14-3-3σ isoform. First, it usually forms a homodimer. Second, 14-3-3σ possesses a ligand-discriminating, special amino acid patch on the second ligand-binding surface (*38*). These findings may explain the difference in the binding properties of 14-3-3β and σ as to CDC25B.

Here, we evaluated whether four other 14-3-3 subtypes (γ, η, θ/τ, and ζ) also bind to CDC25B and exhibit behavior similar to that of 14-3-3β. The 14-3-3θ/τ isoform exhibited slightly different properties from those of the other three isoforms in that it bound to other 14-3-3 motifs in CDC25B in addition to site 309. The 14-3-3ζ isoform bound to CDC25B more weakly at Ser309 than did the other isoforms, except 14-3-3σ. These subtle differences appeared to affect the ability of these isoforms to cause the transfer of CDC25B from the nucleus to the cytoplasm. Our results show that six of the seven 14-3-3 subtypes in mammalian cells behave similarly in terms of CDC25B binding. The specific function of the 14-3-3σ isoform is unknown.

The typical consensus 14-3-3 binding sequence consists of Arg-X-X-Ser/Thr-X-P (mode-I) or Arg-X-X-X-Ser/Thr-X-P (mode-II), where the serine or threonine must be phosphorylated (*39*, *40*). In addition to these binding motifs, 14-3-3 also binds to the recently identified mode-III motif, which consists of (p)S/T-X_{1-2}-COOH at the C-terminus of several proteins (*41*). Although the results of oriented peptide analysis suggest that the Arg-X-X-(p)Ser/Thr-X-P mode-I motif is sufficient for 14-3-3 binding, a more complicated situation appears to exist *in vivo*. For example, we previously found that CDC25B contains five 14-3-3 binding motifs, but only three of these are functional. The principal 14-3-3 binding site is at Ser309, and the Ser216 site in combination with the Ser137 or Ser309 site may also be important, especially for binding to 14-3-3σ.

One possible reason for the apparent non-functionality of certain 14-3-3 binding motifs *in vivo* may be the lack of phosphorylation of target Ser/Thr. The results described in this report suggest another somewhat unexpected explanation. We found that alterations in amino acids C-terminal to the binding motif at site 309 severely impaired 14-3-3 binding, indicating that 14-3-3 binding depends not only on the consensus sequence but also on its context. Thus, the binding of 14-3-3 may require not only the presence of the binding motif in its appropriately phosphorylated form but also the presence of a suitable sequence C-terminal to the binding site. Substitution mutations of amino acid residues often disrupt the local structure of proteins. Therefore, some mutants examined in this study may harbor a structural change that abolishes 14-3-3 binding. However, Ser309 in each CDC25B mutant, except Pro317Ala, was efficiently phosphorylated at the same level as that of the wild-type protein in transfected cells. These results imply (but do not prove unequivocally) that a gross structural change should not be introduced by the mutations. Studies using an oriented peptide library with a random amino acid sequence placed C-terminal to the consensus site will be important for confirmation of our hypothesis.

The specific kinases that phosphorylate Ser309 of CDC25B have yet to be identified. We examined kinases that have been reported to phosphorylate this residue, but they exhibited essentially the same specificity toward mutated substrates *in vitro*. All of the tested kinases required a proline at residue 317 and an arginine at residue 306, although Pro317 was not essential for Ser309 phosphorylation *in vivo*. The kinase responsible for regulating CDC25B localization must exhibit an appropriate subcellular localization. In the normal cell cycle, CDC25B is located in the nucleus, and Ser309 is phosphorylated to some degree even in the absence of cellular injury (*23*). In view of this, kinases that phosphorylate Ser309 would also be expected to be located in the nucleus. Of these kinases, we propose that CHK1 and MK2 may be suitable for the phosphorylation of Ser309 of CDC25B1, even in the absence of specific cellular damage, since they are activated at low levels during DNA replication and environmental stress, respectively (Ref. *26* and our unpublished data). It is a matter for further investigation

as to whether these kinases phosphorylate this site more heavily when cells are injured.

We thank S. Elledge for the generous gift of the plasmids. This work was supported by Grants-in-Aid for Scientific Research from and by the Third-Term Comprehensive 10-Year Strategy for Cancer Control of the Ministry of Health, Labour, and Welfare of Japan. This work was also supported by the Collaborative Research Program of the Cancer Institute of Kanazawa University and by the Kanazawa University 21st Century COE Program of the Ministry of Education, Culture, Sports, Science, and Technology of Japan. S. U. was also supported by a fellowship from the Kanazawa University 21st Century COE Program and a Research-Resident Fellowship from the Human Science Foundation of Japan.

REFERENCES

1. Galaktionov, K. and Beach, D. (1991) Specific activation of cdc25 tyrosine phosphatases by B-type cyclins: evidence for multiple roles of mitotic cyclins. *Cell* **67**, 1181–1194
2. Sadhu, K., Reed, S.I., Richardson, H., and Russell, P. (1990) Human homolog of fission yeast cdc25 mitotic inducer is predominantly expressed in G2. *Proc. Natl. Acad. Sci. USA* **87**, 5139–5143
3. Strausfeld, U., Labbe, J.C., Fesquet, D., Cavadore, J.C., Picard, A., Sadhu, K., Russell, P., and Doree, M. (1991) Dephosphorylation and activation of a p34cdc2/cyclin B complex in vitro by human CDC25 protein. *Nature* **351**, 242–245
4. Jinno, S., Suto, K., Nagata, A., Igarashi, M., Kanaoka, Y., Nojima, H., and Okayama, H. (1994) Cdc25A is a novel phosphatase functioning early in the cell cycle. *EMBO J.* **13**, 1549–1556
5. Hoffmann, I., Draetta, G., and Karsenti, E. (1994) Activation of the phosphatase activity of human cdc25A by a cdk2-cyclin E dependent phosphorylation at the G1/S transition. *EMBO J.* **13**, 4302–4310
6. Kumagai, A. and Dunphy, W.G. (1992) Regulation of the cdc25 protein during the cell cycle in Xenopus extracts. *Cell* **70**, 139–151
7. Hoffmann, I., Clarke, P.R., Marcote, M.J., Karsenti, E., and Draetta, G. (1993) Phosphorylation and activation of human cdc25-C by cdc2—cyclin B and its involvement in the self-amplification of MPF at mitosis. *EMBO J.* **12**, 53–63
8. Nishijima, H., Nishitani, H., Seki, T., and Nishimoto, T. (1997) A dual-specificity phosphatase Cdc25B is an unstable protein and triggers p34(cdc2)/cyclin B activation in hamster BHK21 cells arrested with hydroxyurea. *J. Cell Biol.* **138**, 1105–1116
9. Lammer, C., Wagerer, S., Saffrich, R., Mertens, D., Ansorge, W., and Hoffmann, I. (1998) The cdc25B phosphatase is essential for the G2/M phase transition in human cells. *J. Cell Sci.* **111**, 2445–2453
10. Donzelli, M., Squatrito, M., Ganoth, D., Hershko, A., Pagano, M., and Draetta, G.F. (2002) Dual mode of degradation of Cdc25 A phosphatase. *EMBO J.* **21**, 4875–4884
11. Mailand, N., Podtelejnikov, A.V., Groth, A., Mann, M., Bartek, J., and Lukas, J. (2002) Regulation of G(2)/M events by Cdc25A through phosphorylation-dependent modulation of its stability. *EMBO J.* **21**, 5911–5920
12. Chen, M.S., Hurov, J., White, L.S., Woodford-Thomas, T., and Piwnica-Worms, H. (2001) Absence of apparent phenotype in mice lacking Cdc25C protein phosphatase. *Mol. Cell. Biol.* **21**, 3853–3861
13. Lincoln, A.J., Wickramasinghe, D., Stein, P., Schultz, R.M., Palko, M.E., De Miguel, M.P., Tessarollo, L., and Donovan, P.J. (2002) Cdc25b phosphatase is required for resumption of meiosis during oocyte maturation. *Nat. Genet.* **30**, 446–449
14. Ferguson, A.M., White, L.S., Donovan, P.J., and Piwnica-Worms, H. (2005) Normal cell cycle and checkpoint responses in mice and cells lacking Cdc25B and Cdc25C protein phosphatases. *Mol. Cell. Biol.* **25**, 2853–2860
15. Bulavin, D.V., Amundson, S.A., and Fornace, A.J. (2002) p38 and Chk1 kinases: different conductors for the G(2)/M checkpoint symphony. *Curr. Opin. Genet. Dev.* **12**, 92–97
16. Donzelli, M. and Draetta, G.F. (2003) Regulating mammalian checkpoints through Cdc25 inactivation *EMBO Rep.* **4**, 671–677
17. Bartek, J., Lukas, C., and Lukas, J. (2004) Checking on DNA damage in S phase. *Nat. Rev. Mol. Cell. Biol.* **5**, 792–804
18. Sanchez, Y., Wong, C., Thoma, R.S., Richman, R., Wu, Z., Piwnica-Worms, H., and Elledge, S.J. (1997) Conservation of the Chk1 checkpoint pathway in mammals: linkage of DNA damage to Cdk regulation through Cdc25. *Science* **277**, 1497–1501
19. Matsuoka, S., Huang, M., and Elledge, S.J. (1998) Linkage of ATM to cell cycle regulation by the Chk2 protein kinase. *Science* **282**, 1893–1897
20. O'Neill, T., Giarratani, L., Chen, P., Iyer, L., Lee, C.H., Bobiak, M., Kanai, F., Zhou, B.B., Chung, J.H., and Rathbun, G.A. (2002) Determination of substrate motifs for human Chk1 and hCds1/Chk2 by the oriented peptide library approach. *J. Biol. Chem.* **277**, 16102–16115
21. Miyata, H., Doki, Y., Yamamoto, H., Kishi, K., Takemoto, H., Fujiwara, Y., Yasuda, T., Yano, M., Inoue, M., Shiozaki, H., Weinstein, I.B., and Monden, M. (2001) Overexpression of CDC25B overrides radiation-induced G2-M arrest and results in increased apoptosis in esophageal cancer cells. *Cancer Res.* **61**, 3188–3193
22. Forrest, A. and Gabrielli, B. (2001) Cdc25B activity is regulated by 14-3-3. *Oncogene* **20**, 4393–4401
23. Bulavin, D.V., Higashimoto, Y., Popoff, I.J., Gaarde, W.A., Basrur, V., Potapova, O., Appella, E., and Fornace, A.J., Jr. (2001) Initiation of a G2/M checkpoint after ultraviolet radiation requires p38 kinase. *Nature* **411**, 102–107
24. Peng, C.Y., Graves, P.R., Thoma, R.S., Wu, Z., Shaw, A.S., and Piwnica-Worms, H. (1997) Mitotic and G2 checkpoint control: regulation of 14-3-3 protein binding by phosphorylation of Cdc25C on serine-216. *Science* **277**, 1501–1505
25. Giles, N., Forrest, A., and Gabrielli, B. (2003) 14-3-3 acts as an intramolecular bridge to regulate cdc25B localization and activity. *J. Biol. Chem.* **278**, 28580–28587
26. Manke, I.A., Nguyen, A., Lim, D., Stewart, M.Q., Elia, A.E., and Yaffe, M.B. (2005) MAPKAP kinase-2 is a cell cycle checkpoint kinase that regulates the G2/M transition and S phase progression in response to UV irradiation. *Mol. Cell* **17**, 37–48
27. Dalal, S.N., Schweitzer, C.M., Gan, J., and DeCaprio, J.A. (1999) Cytoplasmic localization of human cdc25C during interphase requires an intact 14-3-3 binding site. *Mol. Cell. Biol.* **19**, 4465–4479
28. Davezac, N., Baldin, V., Gabrielli, B., Forrest, A., Theis-Febvre, N., Yashida, M., and Ducommun, B. (2000) Regulation of CDC25B phosphatases subcellular localization. *Oncogene* **19**, 2179–2185
29. Graves, P.R., Lovly, C.M., Uy, G.L., and Piwnica-Worms, H. (2001) Localization of human Cdc25C is regulated both by nuclear export and 14-3-3 protein binding. *Oncogene* **20**, 1839–1851
30. Uchida, S., Kuma, A., Ohtsubo, M., Shimura, M., Hirata, M., Nakagama, H., Matsunaga, T., Ishizaka, Y., and Yamashita, K. (2004) Binding of 14-3-3beta but not 14-3-3sigma controls the cytoplasmic localization of CDC25B: binding site preferences of 14-3-3 subtypes and the subcellular localization of CDC25B. *J. Cell Sci.* **117**, 3011–3020
31. Furnari, B., Blasina, A., Boddy, M.N., McGowan, C.H., and Russell, P. (1999) Cdc25 inhibited in vivo and in vitro by checkpoint kinases Cds1 and Chk1. *Mol. Biol. Cell* **10**, 833–845

32. Chen, M.S., Ryan, C.E., and Piwnica-Worms, H. (2003) Chk1 kinase negatively regulates mitotic function of Cdc25A phosphatase through 14-3-3 binding. *Mol. Cell. Biol.* **23**, 7488–7497
33. Uto, K., Inoue, D., Shimuta, K., Nakajo, N., and Sagata, N. (2004) Chk1, but not Chk2, inhibits Cdc25 phosphatases by a novel common mechanism. *EMBO J.* **23**, 3386–3396
34. Guan, K.L. and Dixon, J.E. (1991) Eukaryotic proteins expressed in Escherichia coli: an improved thrombin cleavage and purification procedure of fusion proteins with glutathione S-transferase. *Anal. Biochem.* **192**, 262–267
35. Wang, X., Arooz, T., Siu, W.Y., Chiu, C.H., Lau, A., Yamashita, K., and Poon, R.Y. (2001) MDM2 and MDMX can interact differently with ARF and members of the p53 family. *FEBS Lett.* **490**, 202–208
36. Bradford, M.M. (1976) A rapid and sensitive method for the quantitation of microgram quantities of protein utilizing the principle of protein-dye binding. *Anal. Biochem.* **72**, 248–254
37. Uchida, S., Ohtsubo, M., Shimura, M., Hirata, M., Nakagama, H., Matsunaga, T., Yoshida, M., Ishizaka, Y., and Yamashita, K. (2004) Nuclear export signal in CDC25B. *Biochem. Biophys. Res. Commun.* **316**, 226–232
38. Wilker, E.W., Grant, R.A., Artim, S.C., and Yaffe, M.B. (2005) A structural basis for 14-3-3sigma functional specificity. *J. Biol. Chem.* **280**, 18891–18898
39. Muslin, A.J., Tanner, J.W., Allen, P.M., and Shaw, A.S. (1996) Interaction of 14-3-3 with signaling proteins is mediated by the recognition of phosphoserine. *Cell* **84**, 889–897
40. Yaffe, M.B., Rittinger, K., Volinia, S., Caron, P.R., Aitken, A., Leffers, H., Gamblin, S.J., Smerdon, S.J., and Cantley, L.C. (1997) The structural basis for 14-3-3:phosphopeptide binding specificity. *Cell* **91**, 961–971
41. Ganguly, S., Weller, J.L., Ho, A., Chemineau, P., Malpaux, B., and Klein, D.C. (2005) Melatonin synthesis: 14-3-3-dependent activation and inhibition of arylalkylamine N-acetyltransferase mediated by phosphoserine-205. *Proc. Natl. Acad. Sci. USA* **102**, 1222–1227

Inhibition of peroxisome proliferator-activated receptor gamma activity in esophageal carcinoma cells results in a drastic decrease of invasive properties

Hirokazu Takahashi,[1] Kouji Fujita,[1] Toshio Fujisawa,[1] Kyoko Yonemitsu,[1] Ayako Tomimoto,[1] Ikuko Ikeda,[1] Masato Yoneda,[1] Tomotaka Masuda,[2] Katherine Schaefer,[3] Lawrence J Saubermann,[3] Takeshi Shimamura,[1] Satoru Saitoh,[1] Masashi Tachibana,[4] Koichiro Wada,[2] Hitoshi Nakagama[4] and Atsushi Nakajima[1,5]

[1]Gastroenterology Division, Yokohama City University Graduate School of Medicine, 3-9 Fukuura, Kanazawa-ku, Yokohama, Kanagawa 236-0004; [2]Department of Pharmacology, School of Dentistry, Osaka University, 1-8 Yamadaoka, Suita, Osaka 565-0871, Japan; [3]Section of Gastroenterology, Boston University School of Medicine, Boston, MA, USA; and [4]Biochemistry Division, National Cancer Center Research Institute, 5-1-1 Tsukiji, Chuo-ku, Tokyo 104-0045, Japan

(Received December 19, 2005/Revised April 24, 2006/Accepted May 1, 2006/Online publication June 29, 2006)

Esophageal cancer is difficult to treat because of its rapid progression, and more effective therapeutic approaches are needed. The PPARγ is a nuclear receptor superfamily member that is expressed in many cancers. PPARγ expression is a feature of esophageal cancer cell lines, and in the present investigation, the PPARγ antagonists T0070907 and GW9662 could induce loss of invasion but could not induce growth reduction or apoptosis at low concentrations (<10 mM). A high concentration of antagonists (50 μM) inhibited cell growth and induced apoptosis, but these effects did not explain our result at the low concentration. Morphological change, decreased expression of the cell signaling pathway and inhibition of cancer cell invasion were observed in the low concentration. This suggested that PPARγ antagonists inhibited esophageal cancer cell invasion as well as cell adherence, most likely due to alteration in the FAK–MAPK pathway, and this was independent of apoptosis. These results suggested that PPARγ plays an important role in cancer cell invasion and that it might be a novel target for therapy of esophageal cancer. (*Cancer Sci* 2006; 97: 854–860)

Esophageal cancer is associated with a high mortality rate due to its typically late presentation and rapid progression. For tumors that are not amenable to surgical curative resection, chemotherapy and radiotherapy are commonly applied. But most patients continue to have a poor prognosis, along with an increased morbidity due to treatment-related side-effects.[1] Clearly, new therapies for esophageal cancer are needed.

The nuclear transcription factor PPARγ has recently become a putative therapeutic cancer target for a variety of cancers.[2–4] As PPARγ is mainly expressed in adipose tissue and activation plays a central role in adipocyte differentiation and insulin sensitivity,[5] activating synthethic ligands, TZDs, are commonly used as oral antihyperglycemic agents in control of diabetes mellitus type 2. However, PPARγ is also overexpressed in many tumors, including examples in the esophagus, stomach, breast, lung and colon, suggesting that modulation of PPARγ function might impact on tumor survival.[2–4,6,7] Initial efforts have focused on activation with the TZD ligands, as these have been shown to induce G1 cell cycle arrest in a variety of tumor cell lines.[8,9] However, the results of clinical trials with TZDs have shown modest, if any, benefit.[10,11] With esophageal cancers, PPARγ activation by TZDs in cell lines has been reported to inhibit *in vitro* cell growth and/or induce apoptosis.[12–14]

Several observations suggest that inhibition of PPARγ function might be beneficial in treating neoplasms.[15,16] PPARγ is overexpressed in many cancer cell types, but loss-of-function mutations are rare,[17] suggesting that the receptor is a tumor cell survival factor. The hypothesis that PPARγ function might contribute to carcinogenesis or cancer cell survival is also supported by the observation that in one murine model of colon cancer, PPARγ activation led to an increase in tumor formation.[18,19]

Little is known about inhibition of PPARγ function in esophageal cancer cells. In this study, we investigated the effect of PPARγ inhibition on esophageal cancer cell lines using PPARγ-specific antagonists T0070907 and GW9662 in high (50 μM), low (<10 μM) and very low (<10 μM) concentrations. The PPARγ antagonist could prevent cell attachment to the ECM in high concentrations in our previous studies, however, the effect of PPARγ antagonists in low concentrations was not clear.[20,21] A better understanding of the PPARγ function might lead to it being further utilized for cancer treatment.

Materials and methods

Reagents

The PPARγ-specific antagonists T0070907 and GW9662 were purchased from Cayman Chemical (Ann Arbor, MI, USA) and Sigma Chemical (St Louis, MO, USA), respectively.

[5]To whom correspondence should be addressed.
E-mail: nakajima-tky@umin.ac.jp

Abbreviations: DMEM, Dulbecco's minimum essential medium; ECM, extracellular matrix; Erk, extracellular signal-regulated kinase; FAK, focal adhesion kinase; FITC, fluorescein-isothiocyanate; MAPK, mitogen-activated protein kinase; MTT, 3-(4,5-dimethylthiazol-2-yl)-2,5-diphenyltetrazolium bromide; p-Erk, phosphorylated extracellular signal-regulated kinase; p-FAK, phosphorylated focal adhesion kinase; PPARγ, peroxisome proliferator-activated receptor gamma; TZDs, thiazolizinediones.

doi: 10.1111/j.1349-7006.2006.00250.x

Cell culture

Human esophageal cancer cells (KYSE30, KYSE70, KYSE140) used in this study were obtained from the Human Science Foundation (Osaka, Japan). The histology of KYSE30 was well differentiated, KYSE70 poorly, and KYSE140 moderately. KYSE30 and KYSE70 were maintained in DMEM and KYSE140 in Ham's F12 supplemented with 2% fetal bovine serum. Cultures were maintained at 37°C, with an atmosphere of 5% CO_2 and saturated humidity.

Western blot analysis

Adherent cells were washed in phosphate-buffered saline, and cell extracts were prepared in Laemmli lysis buffer. Protein concentrations were measured using Bio-Rad Protein Assay Reagent (Bio-Rad, Richmond, CA, USA) following the manufacturer's suggested procedure. After electrophoresis of 20 μg aliquots using 10% sodium dodecylsulfate–polyacrylamide gel electrophoresis, proteins were transferred to nitrocellulose membranes (Millipore, Bedford, MA, USA), blocked for 1 h in tris-buffered saline with bovine serum albumin at room temperature, and incubated with primary monoclonal antibody for 1 h. The anti-PPARγ antibody (E-8) was purchased from Santa Cruz Biotechnology (Santa Cruz, CA, USA), anti-pFAK(pY397) from BD Biosciences (San Jose, CA, USA) and anti-p-Erk from Cellsignaling Technology (Beverly, MA, USA). After three washings, the membranes were incubated for 1 h at room temperature with secondary antibody, and immune complexes were visualized using the enhanced chemiluminescence detection kit (Amersham, London, UK) following the manufacturer's procedure.

Immunofluorescence and cell morphology

Cells (5×10^5 per well) were grown on collagen-1 coated glass cover slips in six-well flat bottom plates for 24 h. T0070907 and GW9662 were added and the cells were pre-incubated for 24 h. The cells were fixed with 4% formaldehyde followed by 100% ethanol at −20°C. Permeabilization was carried out with 0.1% Triton-X, and non-specific binding was blocked with 2% normal swine serum. Cells were incubated with antipaxillin monoclonal antibody (BD Biosciences) followed by FITC-labeled secondary antibody. Alexa fluoro 594-conjugated phalloidin (Molecular Probes, Eugene, OR, USA) was used to visualize F-actin. The samples were then mounted with Vectashield (Vector Laboratories, Burlingame, CA, USA) and examined by confocal laser scanning microscopy (Carl Zeiss, Oberkochen, Germany). All experiments were done in triplicate.

Assessment of cell growth

Cell proliferation was measured by MTT assay.[22] KYSE70 cells were plated in 96-well plates at a concentration of 5×10^3 cells in 100 μL of DMEM. After 24 h incubation, the medium was changed with various concentrations of T0070907 and GW9662 added (1–50 μM), and the cells further incubated for 24–72 h. MTT solution (0.5%) was then added to each well. After the plates were incubated for 4 h, 20% sodium dodecylsulfate solution was incubated and absorbance at 595 nm was determined using a microplate reader (Model 550; Bio-Rad). Control wells were treated with dimethylsulfoxide alone. Three independent experiments were carried out.

Apoptosis assay

To evaluate the apoptotic cell death, annexin V staining was carried out using an annexin V–FITC apoptosis detection kit I (Becton Dickinson, San Jose, CA, USA) according to the manufacturer's recommendations. Cells were subsequently analyzed by FACScan flow cytometry (Becton Dickinson).

Transwell invasion assays

In vitro cell invasion was assayed in BD BioCoat Matrigel invasion chambers (24 wells, 8 μm pore size; BD Biosciences). The top chamber was seeded with 5×10^4 KYSE70 cells in DMEM. The bottom chamber was filled with DMEM supplemented with 2% fetal bovine serum as a chemoattractant. Cells were preincubated with T0070907 and GW9662 (1–10 μM) in the top chamber, followed by incubation for 24 h in a humidified tissue culture incubator at 37°C under a 5% CO_2 atmosphere. Noninvasive cells were removed from the upper surface of the membrane with a cotton swab, and cells on the lower surface of the membrane were fixed and stained with toluidine blue and mounted on glass slides. Five random fields/well were counted for quantitation of cell invasion. Triplicate wells were counted for each assay.

Statistical analysis

All results are expressed as means ± standard errors of the mean. Statistical comparisons were made using either Student's *t*-test or Scheffe's method after ANOVA. Differences were considered significant at $P < 0.05$.

Results

Esophageal cancer expresses PPARγ protein

Human esophageal cancer tissues were stained using anti-PPARγ-specific antibody, and the expression was high in area of cancer invasion (Fig. 1a). To test whether inhibiting PPARγ activity affects esophageal cell growth or survival, three esophageal cell lines, KYSE30, KYSE70 and KYSE140, were examined. Western blot analysis revealed differential PPARγ protein expression in each. The expression level of PPARγ was very low in normal mucosa, low in KYSE30 cells (well differentiated), moderate in KYSE140 cells (moderately differentiated) and high in KYSE70 cells (poorly differentiated). As the degree of cell differentiation decreased from well differentiated to poorly differentiated, PPARγ protein expression increased. The expression of PPARγ was increased in esophageal cancer tissues compare with normal esophageal epithelial cells (Fig. 1b). The cell line with the highest expression of PPARγ, KYSE70, was used in subsequent investigations into the inhibitory effect of PPARγ activity.

Treatment with PPARγ antagonists decreases cell adhesion to the ECM

Cells treated with 10 or 50 μM of T0070907 and GW9662 underwent morphological changes by 24 h, but those treated with 1 μM did not undergo any morphological change (Fig. 2). At this time point, most cells were still adherents to the plate. However, rather than becoming the normal elongated shape, they were rounded. This morphological change was not the result of apoptosis in cells treated with

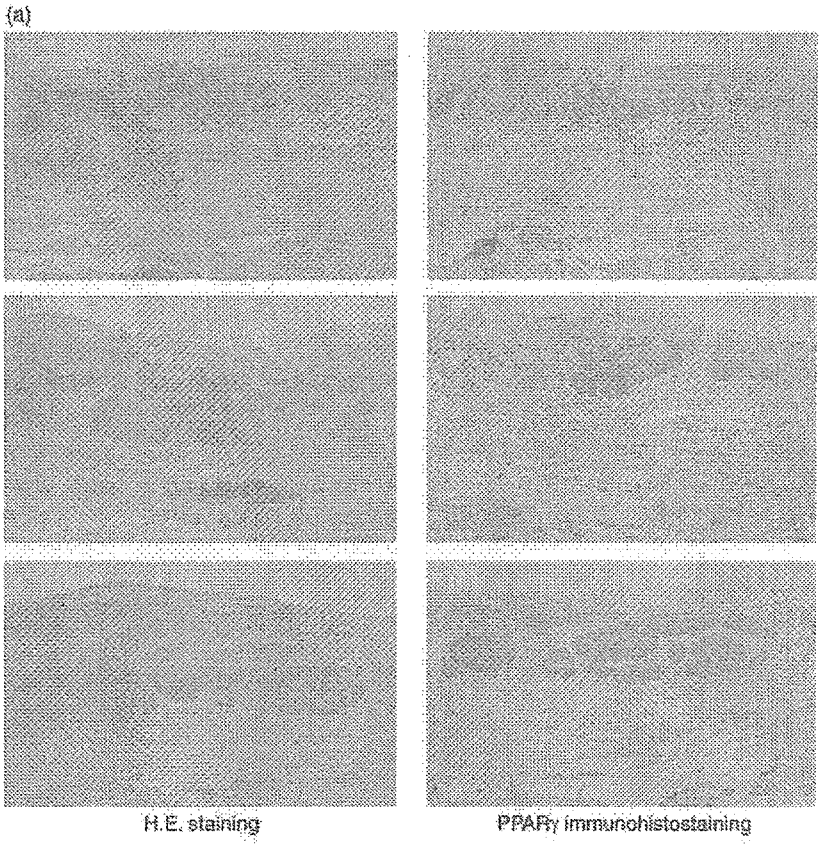

Fig. 1. PPARγ expression in esophageal cancer. (a) Surgical resection of human esophageal cancer tissue stained using HE and antibody specific for PPARγ. The expression was high in area of cancer invasion. (b) The expression level of PPARγ was very low in normal mucosa, low in KYSE30 cells (well differentiated), moderate in KYSE140 cells (moderately differentiated) and high in KYSE70 cells (poorly differentiated). As the degree of cell differentiation decreased from well differentiated to poorly differentiated, PPARγ protein expression increased.

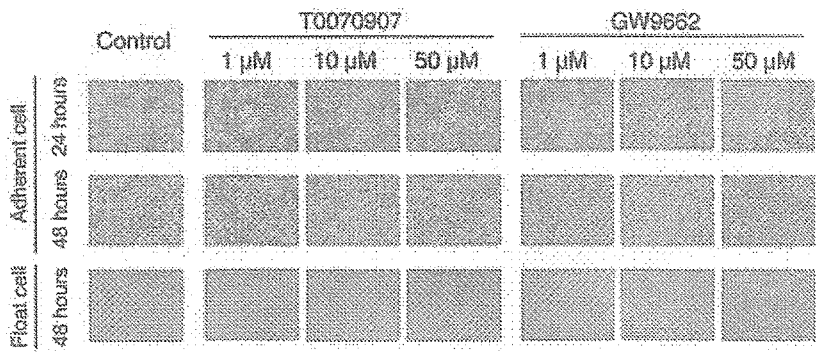

Fig. 2. Morphological changes in esophageal cancer cell lines induced by PPARγ antagonists. KYSE70 cells were incubated with dimethylsulfoxide (control), and 1–50 μM T0070907 and GW9662. Cells treated with 10 and 50 μM of PPARγ antagonists underwent morphological changes by 24 h. By 48 h, 10 μM induced morphological changes but did not inhibit cell adherence; 50 μM induced morphological changes and inhibited cell adherence.

10 μM T0070907 and GW9662, as cells at this time point were not positive for annexin V (Fig. 3). By 48 h, almost half of the cells treated with 50 μM T0070907 and GW9662 were nonadherent. In other words, 1 μM of antagonists induced no change, 10 μM induced morphological changes but did not inhibit cell adherence, and 50 μM induced morphological changes and inhibited cell adherence.

PPARγ antagonists induce change of actin organization

Actin fibers play an important role in maintaining the cytoskeletal structure, and paxillin is functionally important in transducing intracellular messages that are associated with growth factor signaling and cell–ECM interactions.[23] To determine whether the observed cell rounding was associated with alterations in cytoskeletal function, these proteins were

doi: 10.1111/j.1349-7006.2006.00250.x

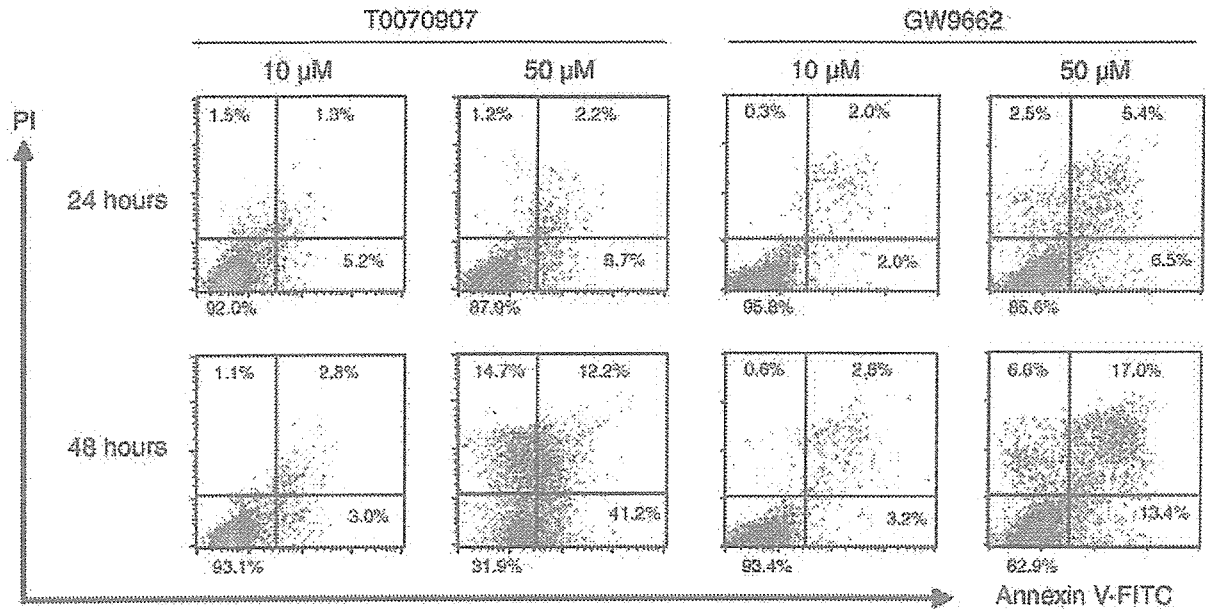

Fig. 3. PPARγ antagonists induced apoptosis in KYSE70 esophageal cancer cells at 48 h. Cells were incubated with 10 and 50 μM T0070907 and GW9662, followed by flow cytometry analysis using annexin V and propidium iodide double staining. Apoptotic cells were observed in 50 μM antagonists at the 48 h time point, but not in 10 μM.

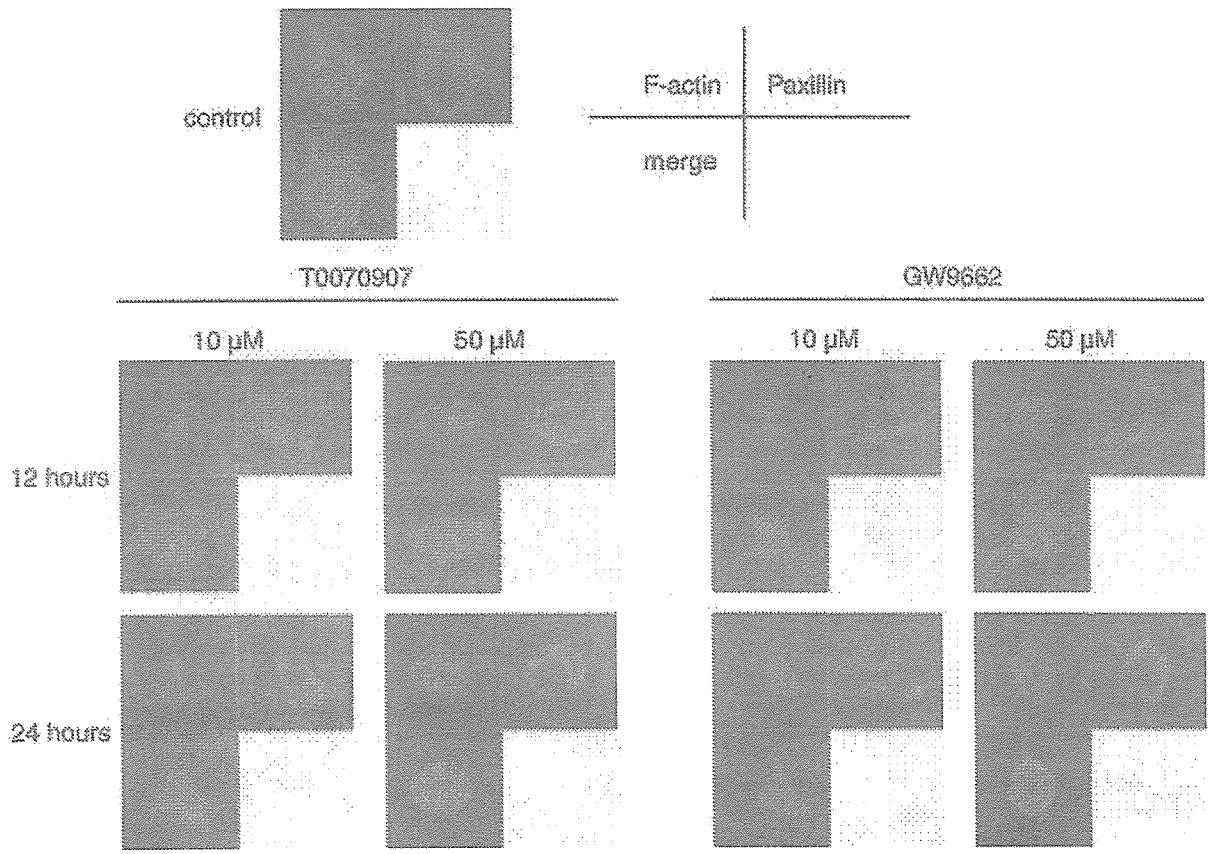

Fig. 4. Before PPARγ antagonist treatment of KYSE70 esophageal cancer cells, actin fibers and paxillin were visible. After 12 h of treatment with 10 and 50 μM T0070907 and GW9662, the cells began to lose their actin fibers, and by 24 h almost all of the cells had changed to a round shape with complete loss of actin fibers.

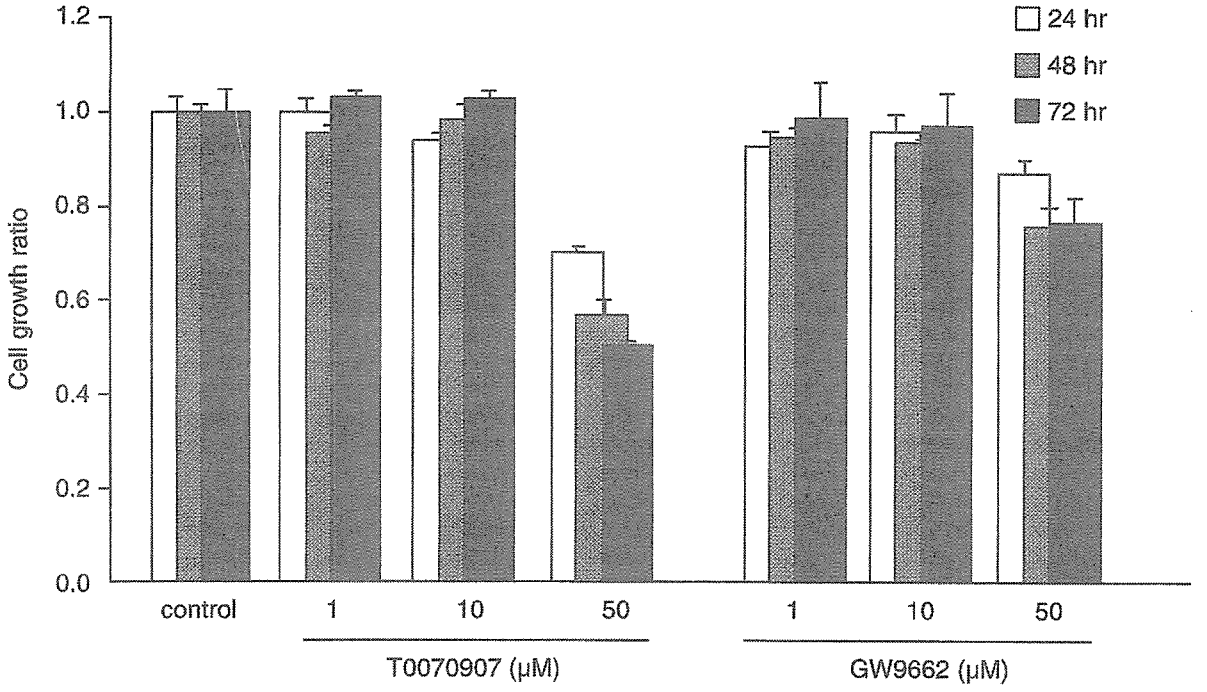

Fig. 5. The PPARγ antagonists T0070907 and GW9662 prevented cell growth in KYSE70 esophageal cancer cells. MTT assay showed the cell growth ratio was significantly reduced in cells treated with 50 μM PPARγ antagonists, and this effect was time-dependent. PPARγ antagonists at concentrations below 10 μM did not reduce the cell growth ratio.

examined by confocal microscopy. Before antagonist treatment, actin fibers and paxillin were visible (Fig. 4). After 12 h of treatment in 10 and 50 μM PPARγ antagonists, the cells began to lose their actin fibers, and by 24 h almost all the KYSE70 cells had changed to a round shape with loss of actin fibers. Similar results were obtained with KYSE30 and KYSE140 cells (data not shown).

Effect of PPARγ antagonists on cell growth

In order to compare the effects of PPARγ antagonism on esophageal cancer cell growth, KYSE70 cells were incubated with T0070907 and GW9662. At 24, 48 and 72 h, the number of cells was measured using MTT assay (Fig. 5). The results were similar in all cell lines, therefore we used KYSE70 cells because they had the highest expression of PPARγ. The compounds did not reduce the growth ratio at concentrations below 10 μM, but did at 50 μM.

Effect of PPARγ antagonists on apoptotic cell death

The results of propidium iodide–annexin V–FITC staining showed that the PPARγ-specific antagonists both induced apoptosis in KYSE70 cells by 48 h at a concentration of 50 μM (Fig. 3), but did not induce apoptosis at 10 μM.

PPARγ antagonism affects the ability of esophageal cancer cell invasion

The PPARγ antagonists had the potential to decrease cell invasiveness. In transwell invasion assays, the number of invasive KYSE70 cells significantly decreased with antagonist treatment below 10 μM, and this effect dose-dependent (Fig. 6). At this concentration (10 μM), the PPARγ antagonists did not induce apoptosis, suggesting that the effect of invasion reduction was independent of apoptosis.

PPARγ antagonism inhibits the phosphorylation of FAK and Erk

To determine possible mechanisms of the cell growth inhibition by PPARγ antagonism, important adhesion and survival cell signaling pathways were investigated. PPARγ antagonists altered FAK (Tyr397) and Erk phosphorylation. KYSE70 cells were incubated with 10 μM of each antagonist.

The results of Western blot analysis revealed decreased expression of p-FAK and p-Erk by the treatment with the antagonists (Fig. 7). p-FAK decreased after 9 h and p-Erk decreased after 12 h.

Discussion

Currently, there is very little information about the inhibition of PPARγ in cancer cells, including esophageal cancer cells. Our previous studies using hepatocellular carcinoma and tongue cancer cells have demonstrated that PPARγ antagonists (high concentration, 50 μM) could prevent cell attachment to ECM, leading to loss of adhesion-induced apoptosis.[20,21] Tongue and esophageal cancer are similar in that they are both squamous cell carcinomas, but the treatment approaches are different. However, esophageal cancer is clinically very important because its mortality rate is very high.

In this study, we demonstrated using esophageal cancer cells that a very low concentration (<10 μM) of PPARγ

doi: 10.1111/j.1349-7006.2006.00250.x

antagonists could induce the inhibition of invasive properties, but not induce growth reduction or apoptosis. MTT assay (Fig. 5) showed that a low and very low concentration of PPARγ antagonists did not inhibit the growth ratio, even after 72 h. Similarly, a low concentration (10 μM) of PPARγ antagonists did not induce apoptosis (Fig. 3). However, a low concentration of PPARγ antagonists could inhibit the cancer cell invasion in the transwell migration assays (Fig. 6). These results suggested that the mechanism by which the PPARγ antagonists inhibited the cancer cell invasion at low concentrations was different from the mechanism by which the high concentration induced apoptosis and cell growth reduction. Therefore, our results suggested that PPARγ might play an important role in cancer cell invasion.

Several reports have clearly demonstrated that PPARγ agonist ligands, the TZDs, could inhibit cell growth and apoptosis of adenocarcinomas, as well as esophageal cancer tissues.[14,24–26] The PPARγ antagonists T0070907 and GW9662 could induce a very similar inhibition of cell growth at a high concentration (50 μM) (Fig. 4). Although it appears paradoxical that both over-activation and inhibition of PPARγ activity could lead to reduced cell growth, this might be a result of different mechanisms. In the TZD setting, a well-recognized G0–G1 cell cycle arrest occurs. In contrast, with PPARγ antagonists, apoptosis appeared to follow loss of adhesion, which was not observed using TZDs. It is suggested that both PPARγ antagonists and TZDs should be considered important candidates for further development as anticancer agents.

PPARγ antagonists were found to first affect cell morphology, with almost all cells changing their cytoskeletal structure, involving both actin fibers and paxillin, within the first 12 h. After adopting a rounded shape, the cells then began detaching from the ECM by 24 h. At this time point, the cells were clearly not apoptotic, as determined by flow cytometric analysis in low concentration (10 μM). This suggested there were different mechanisms dependent on PPARγ activity.

FAK, a 125 kDa non-receptor tyrosine kinase, is an important regulator of cell survival, invasion, migration, and cell cycle

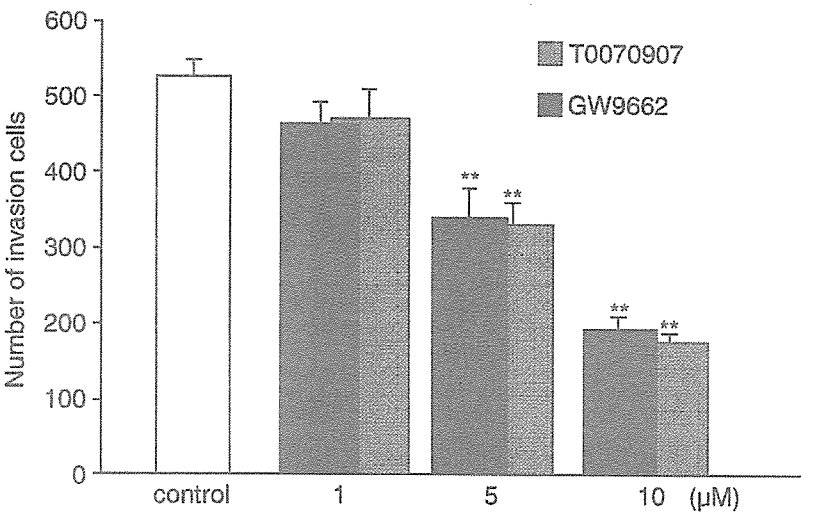

Fig. 6. KYSE70 esophageal cancer cells were incubated with PPARγ antagonists for 24 h during a transwell invasion assay. The number of invasive cells was decreased with antagonist treatment below 10 μM, and this effect was dose-dependent. Error bars represent standard errors of the mean for three replicates. *$P < 0.05$, **$P < 0.01$.

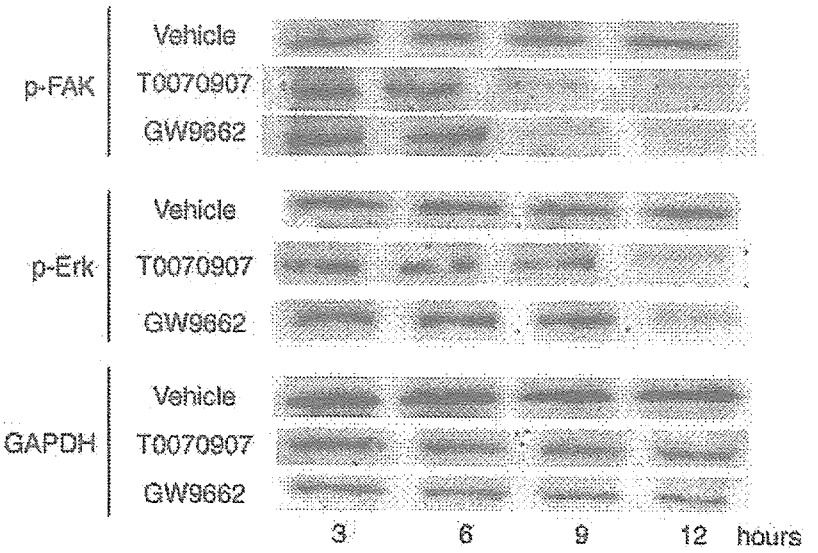

Fig. 7. Expression of FAK (Tyr397) and Erk phosphorylation was altered in KYSE70 esophageal cancer cells incubated with 10 μM PPARγ antagonists. p-FAK was decreased at 9 h and p-Erk was decreased at 12 h.

progression.[27–29] This overexpression of FAK has been observed in a number of human malignant cells, and this might play an important role in determining cellular invasion and metastasis.[30,31] FAK is functionally important in transducing intracellular messages associated with growth factor signaling, cell–ECM interactions, modifying the cytoskeleton and activating MAPK cascades, including Erk. In the present study, the inhibition of phosphorylation of FAK in KYSE70 cells treated with antagonists (10 μM) was observed at 9 h, followed by a reduction in Erk phosphorylation at 12 h. Inhibition of Erk phosphorylation occurred after the inhibition of FAK phosphorylation by PPARγ antagonists, suggesting that PPARγ might play an important role in the MAPK pathway.

High concentration (50 μM) PPARγ antagonists induced apoptosis and cell detachment, and reduced cell growth, but a low concentration (10 μM) could reduce cell invasion and alter the MAPK signaling pathway. These results suggest that the effects of a low concentration of antagonists were independent of the effects of apoptosis, detachment and cell growth inhibition. One study has reported that the difference in effect depends on PPARγ concentration,[32] but further investigation is necessary.

In summary, PPARγ antagonists inhibited esophageal cancer cell invasion as well as cell adherence to ECM, most likely due to alteration in the FAK–MAPK pathway, and this was independent of apoptosis. Our results suggest that PPARγ plays important roles in cancer cell invasion, therefore it might be a novel target for esophageal cancer therapy.

Acknowledgments

This work was supported by a Grants-in-Aid for the Third Term Comprehensive Control Research for Cancer from the Ministry of Health, Labour, and Welfare of Japan, and the Ministry of Education, Science, Sports, Culture, Japan.

References

1 Blazeby JM, Alderson D, Farndon JR. Quality of life in patients with oesophageal cancer. *Recent Results Cancer Res* 2000; **155**: 193–204.
2 Takashima T, Fujiwara Y, Higuchi K *et al.* PPAR-gamma ligands inhibit growth of human esophageal adenocarcinoma cells through induction of apoptosis, cell cycle arrest and reduction of ornithine decarboxylase activity. *Int J Oncol* 2001; **19**: 465–71.
3 Chang TH, Szabo E. Induction of differentiation and apoptosis by ligands of peroxisome proliferator-activated receptor gamma in non-small cell lung cancer. *Cancer Res* 2000; **60**: 1129–38.
4 DuBois RN, Gupta R, Brockman J, Reddy BS, Krakow SL, Lazar MA. The nuclear eicosanoid receptor, PPARgamma, is aberrantly expressed in colonic cancers. *Carcinogenesis* 1998; **19**: 49–53.
5 Desvergne B, Wahli W. Peroxisome proliferator-activated receptors: nuclear control of metabolism. *Endocr Rev* 1999; **20**: 649–88.
6 Mueller E, Sarraf P, Tontonoz P *et al.* Terminal differentiation of human breast cancer through PPAR gamma. *Mol Cell* 1998; **1**: 465–70.
7 Sato H, Ishihara S, Kawashima K *et al.* Expression of peroxisome proliferator-activated receptor (PPAR) gamma in gastric cancer and inhibitory effects of PPARgamma agonists. *Br J Cancer* 2000; **83**: 1394–400.
8 Guan YF, Zhang YH, Breyer RM, Davis L, Breyer MD. Expression of peroxisome proliferator-activated receptor gamma (PPARgamma) in human transitional bladder cancer and its role in inducing cell death. *Neoplasia* 1999; **1**: 330–9.
9 Kitamura S, Miyazaki Y, Shinomura Y, Kondo S, Kanayama S, Matsuzawa Y. Peroxisome proliferator-activated receptor gamma induces growth arrest and differentiation markers of human colon cancer cells. *Jpn J Cancer Res* 1999; **90**: 75–80.
10 Debrock G, Vanhentenrijk V, Sciot R, Debiec-Rychter M, Oyen R, Van Oosterom A. A phase II trial with rosiglitazone in liposarcoma patients. *Br J Cancer* 2003; **89**: 1409–12.
11 Kulke MH, Demetri GD, Sharpless NE *et al.* A phase II study of troglitazone, an activator of the PPARgamma receptor, in patients with chemotherapy-resistant metastatic colorectal cancer. *Cancer J* 2002; **8**: 395–9.
12 Hashimoto Y, Shimada Y, Itami A *et al.* Growth inhibition through activation of peroxisome proliferator-activated receptor gamma in human oesophageal squamous cell carcinoma. *Eur J Cancer* 2003; **39**: 2239–46.
13 Fujii D, Yoshida K, Tanabe K, Hihara J, Toge T. The ligands of peroxisome proliferator-activated receptor (PPAR) gamma inhibit growth of human esophageal carcinoma cells through induction of apoptosis and cell cycle arrest. *Anticancer Res* 2004; **24**: 1409–16.
14 Rumi MA, Sato H, Ishihara S, Ortega C, Kadowaki Y, Kinoshita Y. Growth inhibition of esophageal squamous carcinoma cells by peroxisome proliferator-activated receptor-gamma ligands. *J Lab Clin Med* 2002; **140**: 17–26.
15 Martelli ML, Iuliano R, Le Pera I *et al.* Inhibitory effects of peroxisome poliferator-activated receptor gamma on thyroid carcinoma cell growth. *J Clin Endocrinol Metab* 2002; **87**: 4728–35.
16 Panigrahy D, Shen LQ, Kieran MW, Kaipainen A. Therapeutic potential of thiazolidinediones as anticancer agents. *Expert Opin Invest Drugs* 2003; **12**: 1925–37.
17 Posch MG, Zang C, Mueller W *et al.* Somatic mutations in peroxisome proliferator-activated receptor-gamma are rare events in human cancer cells. *Med Sci Monit* 2004; **10**: BR250–254.
18 Lefebvre AM, Chen I, Desreumaux P *et al.* Activation of the peroxisome proliferator-activated receptor gamma promotes the development of colon tumors in C57BL/6J-APCMin/+ mice. *Nat Med* 1998; **4**: 1053–7.
19 Saez E, Tontonoz P, Nelson MC *et al.* Activators of the nuclear receptor PPARgamma enhance colon polyp formation. *Nat Med* 1998; **4**: 1058–61.
20 Schaefer KL, Wada K, Takahashi H *et al.* Peroxisome proliferator-activated receptor gamma inhibition prevents adhesion to the extracellular matrix and induces anoikis in hepatocellular carcinoma cells. *Cancer Res* 2005; **65**: 2251–9.
21 Masuda T, Wada K, Nakajima A *et al.* Critical role of peroxisome proliferator-activated receptor gamma on anoikis and invasion of squamous cell carcinoma. *Clin Cancer Res* 2005; **11**: 4012–21.
22 Mosmann T. Rapid colorimetric assay for cellular growth and survival: application to proliferation and cytotoxicity assays. *J Immunol Meth* 1983; **65**: 55–63.
23 Giancotti FG, Ruoslahti E. Integrin signaling. *Science* 1999; **285**: 1028–32.
24 Eibl G, Wente MN, Reber HA, Hines OJ. Peroxisome proliferator-activated receptor gamma induces pancreatic cancer cell apoptosis. *Biochem Biophys Res Commun* 2001; **287**: 522–9.
25 Ohta K, Endo T, Haraguchi K, Hershman JM, Onaya T. Ligands for peroxisome proliferator-activated receptor gamma inhibit growth and induce apoptosis of human papillary thyroid carcinoma cells. *J Clin Endocrinol Metab* 2001; **86**: 2170–7.
26 Shimada T, Kojima K, Yoshiura K, Hiraishi H, Terano A. Characteristics of the peroxisome proliferator activated receptor gamma (PPARgamma) ligand induced apoptosis in colon cancer cells. *Gut* 2002; **50**: 658–64.
27 Chen HC, Appeddu PA, Parsons JT, Hildebrand JD, Schaller MD, Guan JL. Interaction of focal adhesion kinase with cytoskeletal protein talin. *J Biol Chem* 1995; **270**: 16995–9.
28 Sieg DJ, Hauck CR, Ilic D *et al.* FAK integrates growth-factor and integrin signals to promote cell migration. *Nat Cell Biol* 2000; **2**: 249–56.
29 Schaller MD. Biochemical signals and biological responses elicited by the focal adhesion kinase. *Biochim Biophys Acta* 2001; **1540**: 1–21.
30 Agochiya M, Brunton VG, Owens DW *et al.* Increased dosage and amplification of the focal adhesion kinase gene in human cancer cells. *Oncogene* 1999; **18**: 5646–53.
31 Owens LV, Xu L, Dent GA *et al.* Focal adhesion kinase as a marker of invasive potential in differentiated human thyroid cancer. *Ann Surg Oncol* 1996; **3**: 100–5.
32 Yamauchi T, Waki H, Kamon J *et al.* Inhibition of RXR and PPARgamma ameliorates diet-induced obesity and type 2 diabetes. *J Clin Invest* 2001; **108**: 1001–13.

doi: 10.1111/j.1349-7006.2006.00250.x

Carcinogenesis vol.27 no.1 pp.162–169, 2006
doi:10.1093/carcin/bgi205
Advance Access publication August 4, 2005

Strain differences in the susceptibility to azoxymethane and dextran sodium sulfate-induced colon carcinogenesis in mice

Rikako Suzuki*, Hiroyuki Kohno, Shigeyuki Sugie, Hitoshi Nakagama[1] and Takuji Tanaka

Department of Oncologic Pathology, Kanazawa Medical University, 1-1 Daigaku, Uchinada, Ishikawa 920-0293, Japan and [1]Biochemistry Division, National Cancer Center Research Institute, 5-1-1 Tsukiji Chuo-ku, Tokyo 104-0045, Japan

*To whom correspondence should be addressed. Tel: +81 76 286 2211; Fax: +81 76 286 6926; E-mail: rikako@kanazawa-med.ac.jp

We have recently developed a mouse model for colitis-related colon carcinogenesis by a combined treatment with azoxymethane (AOM) and dextran sodium sulfate (DSS) in male ICR mice. However, strain differences in the sensitivity to AOM/DSS-induced colon carcinogenesis in mice have yet to be elucidated. The aim of this study was to determine the presence of any genetically determined differences in sensitivity to our model of colon carcinogenesis in four inbred strains of mice. Male Balb/c, C3H/HeN, C57BL/6N and DBA/2N mice were given a single intraperitoneal injection of AOM (10 mg/kg body wt), followed by 1% DSS (w/v) in drinking water for 4 days, and thereafter they received no further treatment for up to 16 weeks. At the end of the study (Week 18), all mice were killed and a histopathological analysis of their colon was performed. The incidence of colonic adenocarcinoma was 100% with a multiplicity (no. of tumors/mouse) of 7.7 ± 4.3 in the Balb/c mice and 50% with a multiplicity of 1.0 ± 1.2 in the C57BL/6N mice. On the other hand, only a few colonic adenomas, but no adenocarcinomas, developed in the C3H/HeN mice (29% incidence with a multiplicity of 0.7 ± 1.5) and the DBA/2N mice (20% incidence with a multiplicity of 0.2 ± 0.4). The inflammation and immunohistochemical nitrotyrosine-positivity scores of the mice treated with AOM and DSS in the decreasing order were as follows: C3H/HeN > Balb/c > DBA/2N > C57BL/6N and Balb/c > C57BL/6N > C3H/HeN > DBA/2N, respectively. Our results thus indicated the presence of strain differences in the susceptibility to AOM/DSS-induced colonic tumorigenesis. These differences may have been directly influenced by the response to nitrosation stress due to the inflammation caused by DSS.

Introduction

Colorectal cancer (CRC) is one of the most common malignant neoplasms in both sexes (1). In Western countries, this malignancy is one of the most leading causes of cancer deaths (1). In patients with inflammatory bowel disease (IBD), including ulcerative colitis (UC) and Crohn's disease, the risk of CRC development is higher than in the general population (2–5). In sporadic and IBD-related CRC, the expression of inducible nitric oxide synthase and cyclooxygenase-2, both of which are associated with inflammation, has been reported to be elevated (6,7). As a result, inflammation is suggested to play an important role in IBD-related CRC (2).

In our recent series of studies on inflammation-related colon carcinogenesis, we developed a novel model of colitis-related colon carcinogenesis using ICR mice. In this animal model, ICR mice received a single dose of a different colonic carcinogen, consisting of either azoxymethane (AOM) (8), 2-amino-1-methyl-6-phenylimidazo[4,5-*b*]pyridine (9) or 1, 2-dimethylhydrazine (10), followed by a 1-week exposure to 2% dextran sodium sulfate (DSS) in their drinking water, which thus resulted in a high incidence of colonic epithelial malignancy within 20 weeks (8–10). We have previously proposed that the colonic inflammation and nitrosative stress caused by DSS exposure contributes to the development of cryptal dysplasia and neoplasms in the colon (8–10).

AOM is a colonic genotoxic carcinogen that is extensively used for the investigation of large bowel carcinogenesis in rodents (11–13). A synthetic sulfate polysaccharide, DSS, is a non-genotoxic colonic carcinogen that is widely used to produce colitis in rodents, which shares most features with human UC (14–18). It is well known that different strains of mice have different sensitivities to xenobiotic including AOM and DSS (19–28). For example, the Balb/CJ strain is known to be susceptible to AOM (26), whereas, the C3H (29), C57BL/6J (26) and DBA/2 (25) strains are less sensitive to AOM. Regarding the sensitivity to DSS in several mouse strains, Balb/c, C3H/HeJ, and C57BL/6J mice are relatively susceptible to DSS, while DBA/2J mice have been reported to be virtually resistant (27,28). It may therefore be possible that the differences in the genetic background of the mice differently affect the colon carcinogenesis induced by AOM and DSS.

The current study was conducted to determine the different sensitivities to AOM/DSS-induced colon carcinogenesis in four different inbred mouse strains, namely Balb/c, C3H/HeN, C57BL/6N and DBA/2N, by evaluating the incidence and multiplicity of colonic tumors. In addition, an immunohistochemical analysis of nitrotyrosine, a marker of both formation of peroxynitrite (30) and perhaps the inflammation-associated carcinogenesis (31), was done to evaluate whether nitrosative stress is involved in the strain difference sensitivity to AOM/DSS-induced colon tumorigenesis.

Materials and methods

Animals, chemicals and diets

For the study 5-week-old male mice of Balb/c, C3H/HeN, C57BL/6N and DBA/2N strains were obtained from Charles River Japan, (Tokyo, Japan). AOM was purchased from the Sigma-Aldrich (St Louis, MO). DSS with a molecular weight of 36 000–50 000 was purchased from ICN Biochemicals,

Abbreviations: AOM, azoxymethane; CRC, colorectal cancer; CYP, Cytochrome P450; DSS, dextran sodium sulfate; IBD, inflammatory bowel disease; IKK, IκB kinase; LPS, lipopolysaccharide; UC, ulcerative colitis.